APPLICATIONS OF SPIN RESONANCE TECHNIQUES TO THE STUDY OF RADIATION EFFECTS

C. KIKUCHI, S. YIP, and S. H. CHEN

Department of Nuclear Engineering
The University of Michigan

Papers Based on Lectures Delivered at

The Neutron Physics Conference

Mackinac Island, Michigan

June 12-17, 1961

The Neutron Physics Conference of 1961 was sponsored by the

UNITED STATES ATOMIC ENERGY COMMISSION,

LEAR, INCORPORATED,

DETROIT EDISON COMPANY,

CONDUCTRON CORPORATION,

and by the

INSTITUTE OF SCIENCE AND TECHNOLOGY,

ENGINEERING SUMMER CONFERENCE PROGRAM,

and MICHIGAN MEMORIAL PHOENIX PROJECT

of THE UNIVERSITY OF MICHIGAN.

These studies were supported in part by a grant

from the NATIONAL AERONAUTICS AND SPACE ADMINISTRATION.

CONTENTS

INTRODUCTION

Since the pioneering investigations by E. Zavoisky[1] and by R. L. Cummerow and D. Halliday[2], the phenomenon of electron spin resonance has been applied to a wide range of fields, varying from the measurement of nuclear spins and magnetic moments to the detection of microwave radiation from Saturn using the ruby maser[3]. The electron spin resonance technique has also been successfully applied to a variety of problems in radiation solid-state physics. However, the research contributions have come from investigators working in different laboratories, and to our knowledge, no one has so far attempted to explore systematically the usefulness of electron spin resonance as a tool for the study of radiation effects, and, at the same time, to present the fundamentals to those who are not familiar with the technique.

The paper is presented in two parts, the first part dealing with the fundamentals of the solid-state Zeeman effect, and the second part concerned with the applications of the phenomenon to certain select examples. We wish to emphasize that our paper is not intended as a survey. Rather, examples which we felt would most clearly illustrate the usefulness of electron spin resonance as a research tool in radiation solid-state physics were selected for detailed discussion.

Part A

THE SOLID-STATE ZEEMAN EFFECT*

In this section some fundamental concepts of spin resonance are presented with intention to promote basic understanding rather than to display completeness and details. It is well known that the energy-level structure of an atomic system depends quite sensitively upon the electric and magnetic fields present in the system. Then, by inducing and observing appropriate transitions between different levels, it should be possible to derive quantitative information regarding the electrons and nuclei, as well as the surroundings of the atoms. In spin resonance, the transitions between levels corresponding to different spin orientations are studied.

In order to make clear the relation of electron spin resonance effects discussed in this paper with the more familiar optical spectroscopy, consider the energy levels of a sodium atom. The three lowest electron states are shown in Figure 1. The well-known yellow lines of sodium, called the D-lines, result from the transitions from the $^2P_{3/2}$ and $^2P_{1/2}$ states to the ground state $^2S_{1/2}$. These are electric dipole transitions for which the selection rules are $\Delta L = \pm 1$. Consider next the effect of a magnetic field. Then, the levels will be split into 4, 2, and 2 levels for the $P_{3/2}$, $P_{1/2}$, and $S_{1/2}$ states, respectively. Each of the sodium D-lines will split into a number of components. However, these components are spaced closely together so that precision measurement of the spacings would be very

*Contributed by C. Kikuchi and S. Yip.

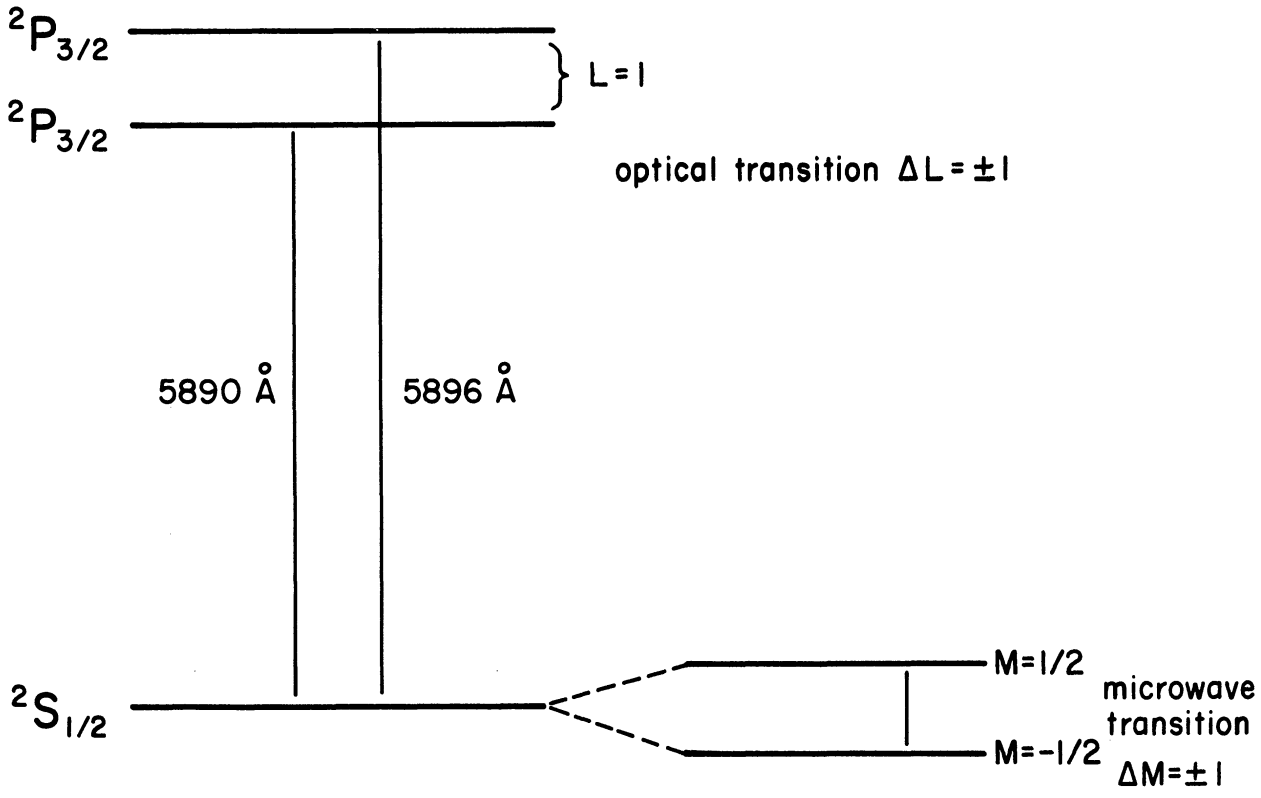

FIG 1

OPTICAL AND MICROWAVE TRANSITIONS IN SODIUM

difficult to make. The usefulness of microwave spectroscopy using electron spin resonance stems from the fact that it is possible, under appropriate conditions, not only to make precision measurement of the splitting of the ground level in a magnetic field, but also at the same time to make precision measurement of effects arising from the much smaller nuclear magnetic moment and electric quadrupole moment.

I. The Spin Resonance Phenomenon. We first discuss qualitatively the phenomenon of spin resonance. It will be seen that a great deal of basic features can be understood on the basis of elementary arguments. The actual problem is, of course, necessarily complicated and requires rather lengthy discussions.

In order for spin resonance transitions to take place it is clear that the system must have non-vanishing resultant spin angular momentum. That is to say, at least one electron in the system has an unpaired spin. All diamagnetic substances with full, closed shells in which pairing of electrons results in zero orbital and spin angular momenta therefore cannot be used in spin resonance studies. Chemical binding in solids, such as ionic or covalent, generally leaves no unpaired electrons in the structure, except when bonds are altered as in irradiation.[4] Among the substances with resultant spin angular momentum the group that has been studied most extensively consists of the iron group transition elements, i.e., Ti, V, Cr, Mn, Fe, Co, Ni, and Cu; these atoms have partially filled inner 3d shells. The reason for this is that electrons prefer the lower energy states of

the outer 4S shells, consequently at least one of the 3d electrons is unpaired.

Under the influence of an externally applied magnetic field the (2S + 1)-fold spin degeneracy is completely removed.* That is to say, there will be 2S + 1 distinct energy levels where S is the electronic spin, being 1/2 if only one electron is unpaired. The process responsible for the splitting is simply the magnetic dipole interaction $-\underline{\mu}\cdot\underline{H}$, where $\underline{\mu}=-g\beta\underline{S}$ is the magnetic moment of the electron. Here $\underline{S}$ is the spin operator, g and β are respectively the gyromagnetic ratio and Bohr magneton. The magnetic energies of the system are $g\beta HM$, where M is the projection of $\underline{S}$ along $\underline{H}$, the axis of quantization, and can assume 2S+1 values from S to -S in integral steps. Physically, the spin angular momentum vector can be pictured as merely precessing about $\underline{H}$ with angular frequency $\nu=g\beta H/h$; its projection along $\underline{H}$ can have any one of the M values. When the system is in thermodynamic equilibrium the probability that the spin vector will have a given orientation is governed by the Boltzmann factor $e^{-E/kT}$, where k is Boltzmann constant. Since $E=-\underline{\mu}\cdot\underline{H}$, the state corresponding to -M therefore will have the greatest population whereas that corresponding to M will have the least.

---

*In zero magnetic field spin degeneracy can be partially removed by effects due to the crystalline electric field.

The magnetic field which causes the Zeeman splittings is a steady D. C. field, and hence cannot induce any transitions. To induce transitions, a microwave radiation is directed at the paramagnetic substance so that the incident, oscillating magnetic field vector $\underline{H}'(t)$ is perpendicular to $\underline{H}$. The effect of the oscillating field is seen by considering it as resolved into two circularly polarized components, one of which precesses about $\underline{H}$ in the same manner as $\underline{S}$. When the frequency of $\underline{H}'(t)$ is not equal to ν there is essentially no effect on S; however, when resonance condition is achieved $\underline{S}$ and the circulating field both precess with frequency ν ; there then exists a coupling on $\underline{S}$, causing it to change its orientation, i.e., $\underline{S}$ makes a transition and assumes one of the other quantized positions with respect to $\underline{H}$. We will later show that this transition is given by the selection rule $\Delta M=\pm 1$. The probability of transition between any two orientations (spin levels) is essentially the same; however, on account of the difference in the population of different energy states the net effect is a transition to a higher energy state of the system with corresponding absorption of micro-wave power.

Let us translate the above remarks into a physical experiment as shown in Figure 2. The paramagnetic sample is located in a cavity which is placed in a steady D. C. magnetic field generated by electromagnets so mounted that the direction as well as the magnitude of the field can be varied. Experimentally, it is much more convenient to hold the frequency of microwave radiation

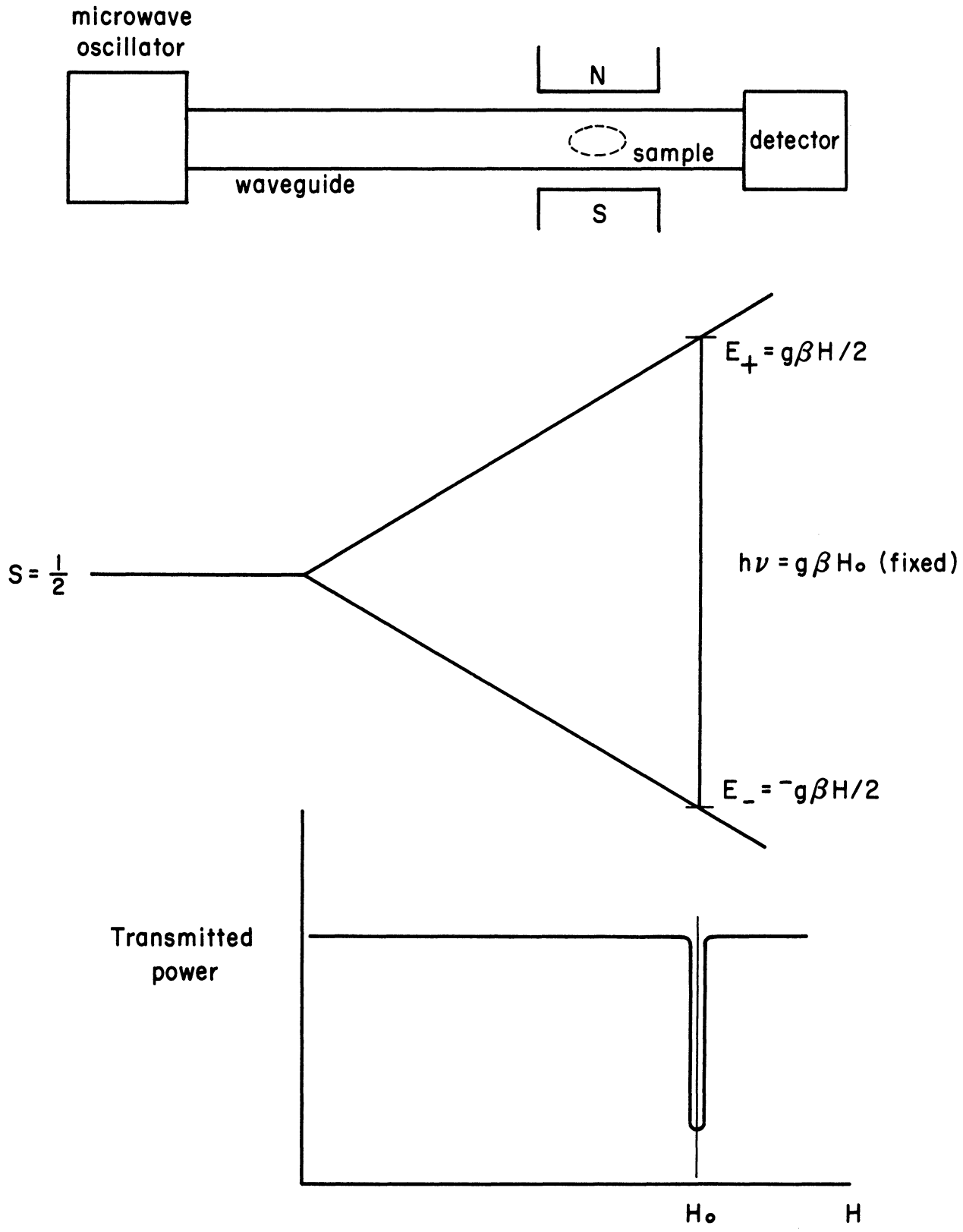

FIG. 2
A SIMPLIFIED ESR EXPERIMENT

constant and vary the magnetic field in approaching a resonance condition. Consequently, a sweeping device is used to change the current producing the D. C. field. Although this field now becomes time-dependent it is nevertheless slowly varying when compared to the microwave field, the magnetic component $\underline{H}'(t)$ is still the sole factor in inducing transitions.* The constant power from the oscillator and the change which takes place during resonance, either reflected or transmitted, are measured by silicon diode detectors. A sharp dip is observed as spin transitions are induced and power is absorbed by the sample. In general, for a given S, there will be $2S + 1$ lines in the spectrum whose spacings as well as intensities will be different, giving rise to what is called the fine structure.** The energy gained then causes the sample temperature to increase via spin-lattice coupling.

Thus far, we have neglected any magnetic property of the nucleus. It is known that some nuclei possess a resultant angular momentum $\underline{I}$, and an associated magnetic moment $\underline{\mu}_N = g_N \beta_N \underline{I}$, where g_N and $\beta_N = \beta\left(\frac{m}{M}\right)$ (m, M are masses of electron and proton) are nuclear gyromagnetic ratio and nuclear magneton. The presence of

---

*A small modulating field is often added to the D.C. field in experiments. This can also be neglected in considering time-dependent perturbations.

**As we will see, fine structure also arises as a result of zero-field splittings due to second order spin-orbit coupling effects as well as spin-spin and crystalline field interactions.

$\underline{\mu}_N$ causes each electron spin level to have an additional degeneracy of 2I + 1 corresponding to the same number of possible nuclear orientations. Here I is the nuclear spin quantum number. This degeneracy, however, is also removed under an external magnetic field due to the interaction $-\underline{\mu}_N \cdot \underline{H}$.* Thus each electronic level is further split into 2I + 1 levels. The axis of quantization can still be taken to be along $\underline{H}$ so the magnetic energies are $g\beta HM - g_N\beta_N Hm$, m being the projection of $\underline{I}$ along $\underline{H}$. As we will show later, the incident radiation gives rise to two types of transitions governed by the selection rules, $\Delta M = \pm 1$ $(\Delta m = 0)$ and $\Delta m = \pm 1$ $(\Delta M = 0)$. The second selection rule allows transitions between levels with different nuclear spin orientations. For these levels the energy separation is relatively small and the population of any two neighboring levels does not differ significantly. The intensity of nuclear transition lines, when observed, is therefore expected to be weak. Nevertheless, such transitions can be detected by allowing two resonance conditions to be simultaneously satisfied. An experiment of this type is known as double resonance and is described in the following.

We consider a paramagnetic sample, S = 1/2 and I = 1/2, whose energy levels at a given $\underline{H}$ is shown in Figure 3, along with a relative population of levels. It is to be expected that the

---

*Interaction between nuclear and electronic spins also removes the degeneracy. This effect will be considered in later discussions.

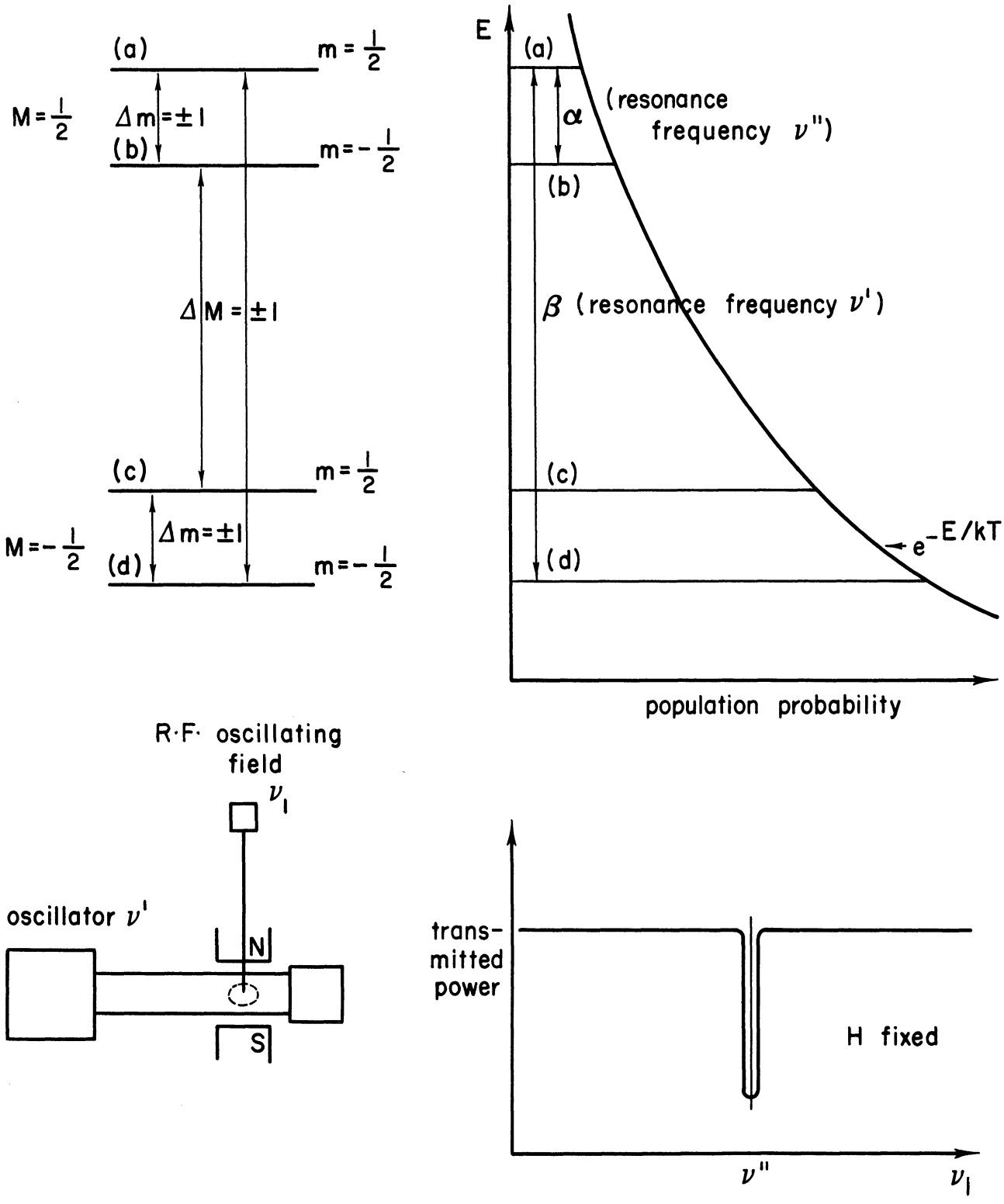

FIG 3
DOUBLE RESONANCE EXPERIMENT

line intensity is more enhanced the greater the difference in population of the levels involved. The intensity of transition α between levels (a) and (b) is ordinarily weak. But if at the same time transition β from (d) to (a) can be induced, then the population of (a) will be greatly increased, resulting in a more intense α line. The experimental modification consists of adding an RF field to the apparatus already shown in Figure 2. The D. C. field is held at a value such that transition β takes place corresponding to an oscillator frequency ν' ; however, the rate of transition begins to decrease in time due to the buildup in population of (a) and depletion of (d). Then the RF frequency is varied until transition α occurs. This process causes a large decrease of population of (a) and results in a renewed absorption line corresponding to an increased β transition rate. Alternatively, a RF detector may be used which then measures the sharp peak resulting from transitions between nuclear levels.

The electronic transition according to the selection rule $\Delta M = \pm 1 \ (\Delta m = 0)$ is the transition ordinarily measured in electron spin resonance. On account of nuclear spin each line is now split into 2I + 1 equally spaced lines. This is seen from the effective magnetic field, $\underline{H} + \underline{H}_N$, that interacts with the electron magnetic moment. $\underline{H}_N$, the field due to the nucleus, can have 2I + 1 equally spaced values corresponding to as many nuclear

orientations.* The splitting produces 2I + 1 lines of equal intensity, as probability of population is essentially the same for all nuclear orientations at normal temperatures. Since the separation of these lines is a nuclear effect and is small compared to splittings among electronic levels, the lines will appear as a group, constituting what is called the hyperfine structure.

It is seen that electron spin resonance gives a direct measurement of the nuclear spin. Therefore, such measurements can be used to identify different isotopes in an element. For example, vanadium is essentially 100 per cent V^{51} with I = 7/2, so its spectrum yields groups of eight lines. On the other hand, natural chromium consists of 90 per cent isotopes with I = 0 and about 9.5 per cent of Cr^{53} with I = 3/2. Its spectrum is a strong central line, corresponding to the abundant isotopes, plus four much weaker lines due to Cr^{53}. The spectrum of an element used in this manner is sometimes referred to as the paramagnetic resonance signature.

We have attempted to give a brief description of the spin resonance phenomenon by using simple examples and elementary arguments. While we believe that the illustration is instructive it admittedly represents an oversimplification. For instance,

---

*Axis of quantization for nuclear spin is not necessarily along the magnetic field; this is true only in the strong field case. Ordinarily the field produced by electrons determines the quantization axis.

effects due to crystalline electric field and other perturbations, which are ordinarily present, have been ignored. It is to be expected that consideration of these aspects leads to a considerably more complicated problem; in fact, it has not been possible to solve the general quantum mechanical problem in any rigorous manner. However, there exist several useful approximation methods, some of which we shall now discuss in the following.

II. The Hamiltonian. We begin with a more rigorous examination of the interactions involved in spin resonance. A fundamental and instructive derivation of these interactions is given by Dirac's theory of electrons. The Hamiltonian for a single electron in electric and magnetic fields is first obtained. The interactions of an atomic system placed in a crystalline electric field and subjected to an external magnetic field can then be found by appropriate specifications of fields and potentials and some obvious generalizations.* This has been done in Appendix A. Fortunately, the general Hamiltonian can be simplified since in spin resonance we are primarily interested in the effects of crystalline forces and the magnetic behavior of electrons and nuclei. Furthermore, we need to consider only the electrons in the unfilled shell such as the 3d shell for the iron group transition elements.

---

*Such a treatment necessarily cannot give any interaction which does not include the electron. Interactions involving only the nucleus must appear as additional effects; see Appendix B.

The appropriate Hamiltonian can be exhibited as

(1) $$\mathcal{H} = \mathcal{H}_0 + V + \mathcal{H}_{LS} + \mathcal{H}_{SS} + \mathcal{H}_e + \mathcal{H}_N + \mathcal{H}_n + \mathcal{H}_Q$$

where

$$\mathcal{H}_0 = \sum_i \left(\frac{P_i^2}{2m_0} - \frac{Ze^2}{r_i} + e^2 \sum_k{}' \frac{1}{r_{ik}} \right)$$

$$\mathcal{H}_{LS} = 2Z\beta^2 \sum_i (\underline{l}_i \cdot \underline{s}_i) r_i^{-3}$$

$$\mathcal{H}_{SS} = 2\beta^2 \sum_{i,k}{}' \left\{ (\underline{s}_i \cdot \underline{s}_k) r_{ik}^{-3} - 3 (\underline{s}_i \cdot \underline{r}_{ik})(\underline{s}_k \underline{r}_{ik}) r_{ik}^{-5} \right\}$$

$$\mathcal{H}_e = \beta \underline{H} \cdot \sum_i (\underline{l}_i + 2\underline{s}_i)$$

$$\mathcal{H}_N = 2 g_N \beta_N \beta \underline{I} \cdot \sum_i \left\{ \frac{l_i(l_i+1)}{j_i(j_i+1) r_i^3} \underline{j}_i + \frac{2\delta(r_i)}{3r_i^2} \underline{s}_i \right\}$$

$$\mathcal{H}_n = - g_N \beta_N \underline{H} \cdot \underline{I}$$

$$\mathcal{H}_Q = \frac{e^2 Q}{2I(2I-1)} \sum_i \left\{ I(I+1) r_i^{-3} - 3 (\underline{I} \cdot \underline{r}_i)^2 r_i^{-5} \right\}$$

$$+ \frac{3eQ}{4I(2I-1)} \left(\frac{\partial^2 V}{\partial z^2} \right)_0 \left[I_z^2 - \frac{I(I+1)}{3} \right] .$$

In obtaining (1) from our results in Appendix A we have neglected relativistic correction terms and most of the electron-electron interactions. We have also added the term $\mathcal{H}_n$ and the second term in $\mathcal{H}_Q$, the nuclear terms arising from external effects.* The order in which the various contributions appear indicates their relative importance so far as the orders of magnitude are concerned.

The main term $\mathcal{H}_o$ in (1) is the familiar Hamiltonian of a many-particle system with coulomb interactions. The resulting energy level separation is of order 10^5 cm^{-1} (1 ev = 8,065 cm^{-1}). The interaction of electrons with crystalline electric field is represented by V, the magnitude of which varies considerably.[5] In the case of iron group cyanides it can be greater than the electrostatic interactions among electrons but less than the electron-nuclear term. In the case of iron group salts it assumes the order given in (1), and in the case of rare earth salts it is less important than the spin-orbit interaction. For our consideration V is of order 10^3 - 10^4 cm^{-1} whereas $\mathcal{H}_{LS}$ gives rise to spin-orbit splittings of order 10^2 cm^{-1}. The magnetic interactions among electrons are of order 1 cm^{-1} and can be ignored in general, but spin-spin effects $\mathcal{H}_{SS}$ could be important in

---

*The two terms given in $\mathcal{H}_Q$ have been derived in Appendix B.

Cr^{++}, Mn^{++}, Cr^{+++}[6].* The primary effect of an external magnetic field is given by $\mathcal{H}_e$, the usual interaction with the magnetic moments of the electrons. The resulting Zeeman splittings at normal field strength are of order 1 cm^{-1}. The remaining terms in (1) describe interactions involving nuclear spin, the dominant one being $\mathcal{H}_n$ which represents interactions with the magnetic field produced by the electrons. This effect causes hyperfine splittings which are of order 10^{-2} cm^{-1}. It has been shown in Appendix A that the last term is the sole contribution of s-state electrons. On account of its sharply peaked behavior it is often referred to as the contact interaction, and is responsible for the s-electron effect. The direct interaction of the external magnetic field with nuclear magnetic moment is given by $\mathcal{H}_N$. The resulting splittings are of order 10^{-3} cm^{-1}; although this effect is sufficiently small to be negligible, nevertheless, it produces an asymmetry in the hyperfine structure allowing certain signs to be determined.[5] The two terms representing the interactions of nuclear electric quadrupole moment with the electrons and crystalline field are given by $\mathcal{H}_Q$ (See Appendix B). Usually the effects are of order 10^{-4} cm^{-1}. In obtain-

---

*Note that the other electron-electron interactions such as orbit-orbit and spin-other-orbit have been neglected. Although they are of no interest in spin resonance, recent investigations have shown that these effects disturb the Lande interval rule and are of importance in many spectra; see Slater[7], p. 199.

ing the expressions in $\mathcal{H}_Q$ we have made use of the fact that coordinate variables can be replaced by equivalent angular momentum operators. The constant $Q' = [3eQ/4I(2I-1)](\partial^2 V/\partial z^2)_0$, where Q is the quadrupole moment and the derivative is to be evaluated at the center of mass of the nucleus, measures the strength of the quadrupole interaction.

The above terms therefore constitute the essential interactions encountered in spin resonance studies. Thus far, it has not been possible to solve the general spin resonance problem except by perturbation methods. However, these approximations, which are seldom carried beyond second order, have been found to give satisfactory correlation with experimental measurements.

In applying perturbation theory the unperturbed part is first diagonalized using the self-consistent field method. The total orbital angular momentum $\underline{L} = \sum_i \underline{l}_i$ and the total spin angular momentum $\underline{S} = \sum_i \underline{s}_i$ form a resultant electronic angular momentum $\underline{J} = \underline{L} + \underline{S}$ which causes each energy level, in the absence of electric and magnetic perturbations, to have a degeneracy of $2J + 1$. Next, the crystalline electric field is taken into account. In our case, the perturbation is sufficiently large to decouple $\underline{L}$ and $\underline{S}$, thus M_L and M_S, the quantum numbers of L_Z and S_Z, become good quantum numbers.* (Physically the two angular momenta

---

*This corresponds to the strong field case, or LS coupling. In other extreme cases energy levels are labelled by M_J, the quantum number of J_Z, corresponding to the weak field case (rare earth salts), or jj coupling.

precess separately about the axis of quantization, that of the perturbing electric field.) Moreover, separations between the M_L levels are so large that transitions will be in the optical region.* This implies that in spin resonance the separated M_L levels can be considered isolated; in particular, only the lowest level is of interest since the population of higher levels at normal temperatures is negligible. The lowest level still contains a degeneracy of 2S+1 due to spin. As we will see later, some further splittings may occur on account of the symmetry in the crystalline field. These splittings exist even in the absence of magnetic perturbation, hence they contribute to the so-called zero-field splittings.

The remaining terms in (1) can be treated at the same time. If we proceed to compute the matrix elements of these perturbations with respect to the orbital states only, the result is known as the spin Hamiltonian for it contains only spin operators. Such a Hamiltonian explicitly displays the resonance properties of the system and, when diagonalized, gives the energies arising from the entire perturbation. For illustrative purpose we can take the perturbations as

$$(2)\qquad \mathcal{H}' = \lambda \underline{L}\cdot\underline{S} + \beta \underline{H}\cdot(\underline{L}+2\underline{S}) + A\,\underline{I}\cdot\underline{S} - g_N\beta_N \underline{H}\cdot\underline{I} + Q'\left[I_z^2 - \frac{I(I+1)}{3}\right],$$

*Orbital degeneracy may not be completely removed. For example, in the case of 3d electrons, cubic and tetragonal fields still leave the highest level doubly degenerate.

where we have neglected correlations among the electrons as given by $\mathcal{H}_{ss}$ and electronic interaction with nuclear quadrupole moment.* It will be assumed that the orbital moment is quenched, that is, the ground state is a singlet and the expectation value of L_Z is zero.

To first order the spin Hamiltonian corresponding to $\mathcal{H}'$ is

$$\mathcal{H}'_S = 2\beta \underline{H}\cdot\underline{S} + A\underline{I}\cdot\underline{S} - g_N\beta_N \underline{H}\cdot\underline{I} + Q'\left[I_z^2 - \frac{I(I+1)}{3}\right]. \tag{3}$$

Terms containing $\underline{L}$ vanish because the components of $\underline{L}$ have zero diagonal matrix elements in this approximation. Since $M = M_S$ and $m = M_I$ are good quantum numbers in the unperturbed problem the first order energies become

$$E(M,m) = 2\beta HM + AMm - g_N\beta_N Hm + Q'\left[m^2 - \frac{I}{3}(I+1)\right]. \tag{4}$$

We have seen earlier that $\underline{H}$ consists of two parts, of which the time-dependent $\underline{H}'(t)$ is responsible for inducing transitions. From perturbation theory it is known that transition probability is proportional to the square modulus of matrix elements of $2\beta\underline{H}'(t)\cdot\underline{S} - g_N\beta_N\underline{H}'(t)\cdot\underline{I}$. The second term, being smaller by several orders of magnitude, is customarily neglected so far as transitions are concerned. The spin operator $\underline{S}$ conveniently separates into its components of which only S_x and S_y give non-vanishing matrix elements between states of different M,

---

*More general perturbations have been treated by Abragam and Pryce[6]; see also Bleaney and Stevens[5].

(5) $$\langle M|S_{\pm}|M\mp1\rangle = \left[S(S+1)-M(M\mp1)\right]^{1/2},$$

where $S \pm = S_x \pm i\, S_y$. Therefore, the conventional electron spin resonance experiments (ESR) are characterized by the selection rule $\Delta M = \pm 1$ $(\Delta m = 0)$. However, if transitions among different nuclear spin states can be observed they are then governed by the selection rule $\Delta m = \pm 1$ $(\Delta M = 0)$. With a given selection rule the resonance condition can be readily exhibited using (4). For instance,

$$E(M,m) - E(M-1,m) = h\nu = 2\beta H + A m .$$

The spectrum will show a group of $2I + 1$ lines, and from their separation the hyperfine structure coupling constant A is determined.

To second order in perturbation we need to compute the non-diagonal matrix elements between ground state and all other states. Here only terms in $\underline{L}$ are non-vanishing. The correction to the energy eigenvalue involves the square modulus of these matrix elements and therefore contains quadratic terms of the components of $\underline{H}$ and $\underline{S}$. Hence the spin-Hamiltonian becomes

$$\mathcal{H}_s' = \lambda^2 d_{ij} S_i S_j + \lambda\beta f_{ij} H_i S_j + \beta^2 \Lambda_{ij} H_i H_j + 2\beta \underline{H}\cdot\underline{S}$$
$$+ A\,\underline{I}\cdot\underline{S} - g_N\beta_N \underline{H}\cdot\underline{I} + Q'\left[I_z^2 - \frac{I(I+1)}{3}\right]$$

or

$$\mathcal{H}_S' = \lambda^2 \underline{S}\cdot D\cdot \underline{S} + \beta \underline{H}\cdot g\cdot \underline{S} + A\,\underline{I}\cdot\underline{S} - g_N\beta_N \underline{H}\cdot\underline{I} + Q'\left[I_z^2 - \frac{I(I+1)}{3}\right], \tag{6}$$

where D and g = $2\delta_{ij} + \lambda f_{ij}$ are tensors. The term in $\underline{H}\cdot\lambda\cdot\underline{H}$ has been discarded since it represents a constant energy; consequently it is of no interest. The first term in (6) describes the effect due to spin-orbit coupling which causes zero magnetic field splittings. We will see later that the crystalline field also may produce zero field splittings. The next term gives a generalized Zeeman splitting with possible anisotropy in the spectroscopic splitting factor g arising from the mixture of spin-orbit and magnetic field interactions.* In the presence of a strong crystalline electric field it is seen that the effective perturbations and the resulting resonance properties of the system become angular dependent. In a given calculation it will then be necessary to determine a diagonal coordinate system (axis of quantization) in terms of the angles specifying the external magnetic field with respect to the crystal axes[8,9]. The spin-Hamiltonian, in all cases, must exhibit the same symmetry as that of the crystalline field. For instance, with axial symmetry

---

* This term is diagonal along $\underline{H}$ when g is isotropic; otherwise it is diagonal along $g\cdot\underline{H}$.

$$(7)\qquad \mathcal{H}'_s = \lambda^2 D S_z^2 + \beta\left[g_{\parallel} H_z S_z + g_{\perp}(H_x S_x + H_y S_y)\right] + A I_z S_z + A'(I_x S_x + I_y S_y) - g_N \beta_N \underline{H}\cdot\underline{I} + Q'\left[I_z^2 - \frac{I(I+1)}{3}\right].$$

We note that $g_{\parallel}$ and $g_{\perp}$ give the magnetic field splittings when the field is parallel and perpendicular to the crystalline axis. Similarly, A and A' measure the hyperfine splittings in the parallel and perpendicular directions. The value of S to be used in (7) is an "effective electronic spin", determined by the condition that 2S + 1 is the degeneracy of the lowest level (ground state), and may be different from the free ion value.

It is to be noted that, in principle, constants D, g, A, and Q' may be computed for a given orbital. At the same time, these parameters can be measured. Therefore, although the spin-Hamiltonian is an expression obtained entirely from theoretical considerations it is, nevertheless, a very useful tool relating theory and experiment.

Before closing this section we turn briefly to the crystalline electric field. As two examples we consider fields with axial and cubic symmetries. In the first case, we would expect a dependence of the form $D'(z^2 - r^2/3)$ where z-axis is taken to be the axis of symmetry. The corresponding effect appears in the spin-Hamiltonian as $D\left[S_z^2 - \frac{S(S+1)}{3}\right]$. For the cubic case we would

expect the potential to contain coordinates in even powers of x, y, z and cross terms, all of which must be symmetric in the three variables. In the spin-Hamiltonian lowest order terms constitute $S_x^2 + S_y^2 + S_z^2$, a constant. Next order terms are $S_x^4 + S_y^4 + S_z^4$ and cross terms such as $S_x^2 S_y^2$ etc. The cross terms, however, do not need to appear by virtue of the relation $(S_x^2 + S_y^2 + S_z^2)^2 = S_x^4 + S_y^4 + S_z^4 + (\text{cross terms})$, where the left-hand side is another constant. All higher orders can be reduced in this manner so that a potential with cubic symmetry has the form $\frac{a}{6}(S_x^4 + S_y^4 + S_z^4)$. In Figure 4 we show the spectra for $S = 5/2$ (Mn^{++}, Fe^{+++}). There will be $2S + 1$ spin levels, and therefore $2S$ absorption lines. It is noted that line separations are influenced by crystalline field symmetry whereas the relative intensities, predicted by the matrix elements for S_+ given in (5), remain unchanged.

The above discussions show that quantitative information on the nucleus, electrons, and crystalline field can be obtained by spin resonance experiments. In the following sections we will show how the basic concepts can be extended to the study of radiation effects in solids. A few applications will be considered.

AXIAL FIELD

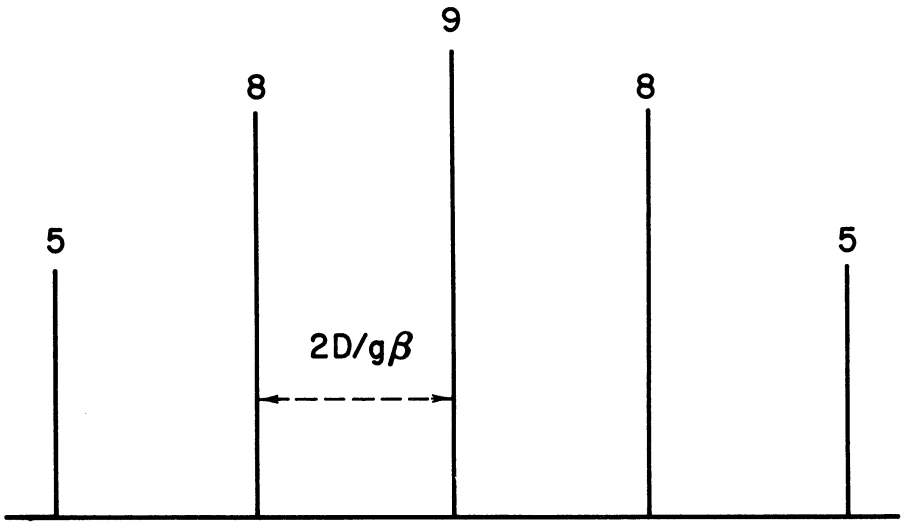

CUBIC FIELD

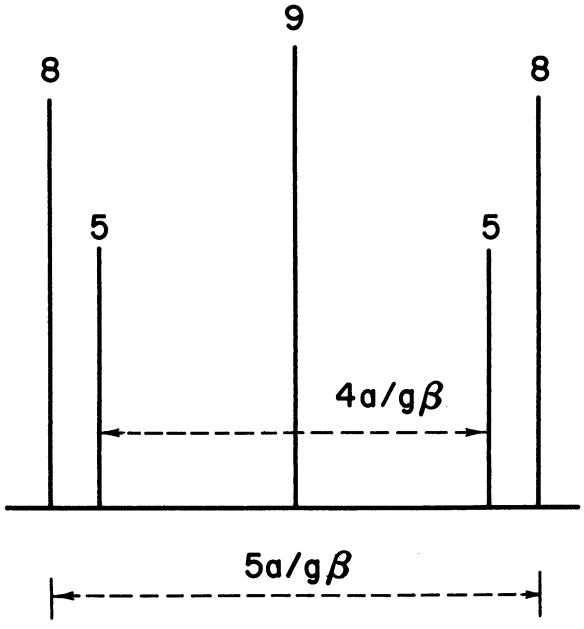

FIG. 4
RESONANCE LINES FOR $S = \frac{5}{2}$ WITH
AXIAL AND CUBIC CRYSTALLINE FIELDS

Part B

APPLICATION OF SPIN RESONANCE TECHNIQUES TO THE STUDY OF RADIATION EFFECTS*

The purpose of this part of the discussion will be to show how spin resonance technique can be used to obtain definitive information about effects produced by nuclear radiations. Furthermore, because the group to whom this is addressed consists primarily of nuclear physicists, emphasis will be placed on those aspects of magnetic resonance that have added to our knowledge about the nucleus. The discussions will be kept as simple as possible in order to stress the physical basis of magnetic resonance. Some calculations will be made to illustrate the use of Spin Hamiltonian, derived in Part I, in correlating the experimental data.

The reason for the usefulness of electron spin resonance stems from the fact that the electrons (for ESR) and the nuclei (for NMR) located in a solid can be thought of as microscopic. The energy of these electrons will be affected by the electric field produced by the charged ions and the magnetic field produced by the nuclei in the volume effectively occupied by the electrons. These electrons may actually occupy an effective volume which includes many atoms.

---

* Contributed by C. Kikuchi and S. H. Chen

In order to show the usefulness of ESR in obtaining the kind of information just mentioned, we shall discuss a few examples in some detail which hopefully can illustrate and elaborate on the fundamental principles discussed in Part A. The examples that have been chosen are:

1) Vacancies in MgO due to Cr impurity.
2) Vacancy in MgO due to neutron irradiation.
3) Neutron cross section measurement by spin resonance.
4) Nuclear moments measurements.
5) Radiation solid-state chemistry.

It should be emphasized that this discussion is not intended as a survey of the field. The above examples are chosen more or less for the interest of nuclear physicists, and furthermore, as we shall see, considerable emphasis will be put on the work that has been or is being carried out at The University of Michigan.

I. Nature of Crystal Structure and Defects in MgO

We shall now show how the theory developed in the preceding section can be used to get definitive information about defects produced in crystalline solids. For this purpose we shall take MgO as an example. This material was picked for various reasons:

1) Simple crystal structure (like NaCl)

   NaCl: $a_o = 5.64\ A^o$

   MgO: $a_o = 4.24\ A^o$

2) Various impurities can be incorporated, such as V, Cr, Mn, Fe, Co, Ni, Cu.

3) Optical properties studies by Hansler and Segelken (1960)[10].

4) Possibility of becoming maser material by neutron irradiation.

MgO crystal is a single crystal with F.C.C. structure like that of NaCl. Each Mg^{++} ion is surrounded by six $O^{=}$ ions located along the crystal axes, forming an octahedral structure (see Figure 5).

For such crystals, the absorption spectrum may be sorted into lines arising from Cr^{+3} substitutional ions in three different electric field symmetries:

1) Cubic symmetry (Octahedral symmetry).

2) Axial symmetry in 100 direction (Tetragonal symmetry).

3) Axial symmetry in 110 direction (see Figure 6).

The formation of the above three symmetries may be pictured as follows: A Cr^{+3} ion replaces a Mg^{++} site, forming a complete cubic symmetry configuration. Owing to an extra charge in Cr^{+3}, a charge compensation has to occur in some way. It is conceivable that this may be done by having a Mg^{++} vacancy somewhere in the lattice site. Such vacancies, while overcompensating for the single extra positive charge of the nearby Cr^{+3} ion with axial symmetry, serve to help compensate for the many extra Cr^{+3} ions in a purely cubic electric field. This mechanism supports the fact that experimentally a strong central line for Cr^{+3} in a cubic crystalline field is observed. The axial symmetry of cases (2)

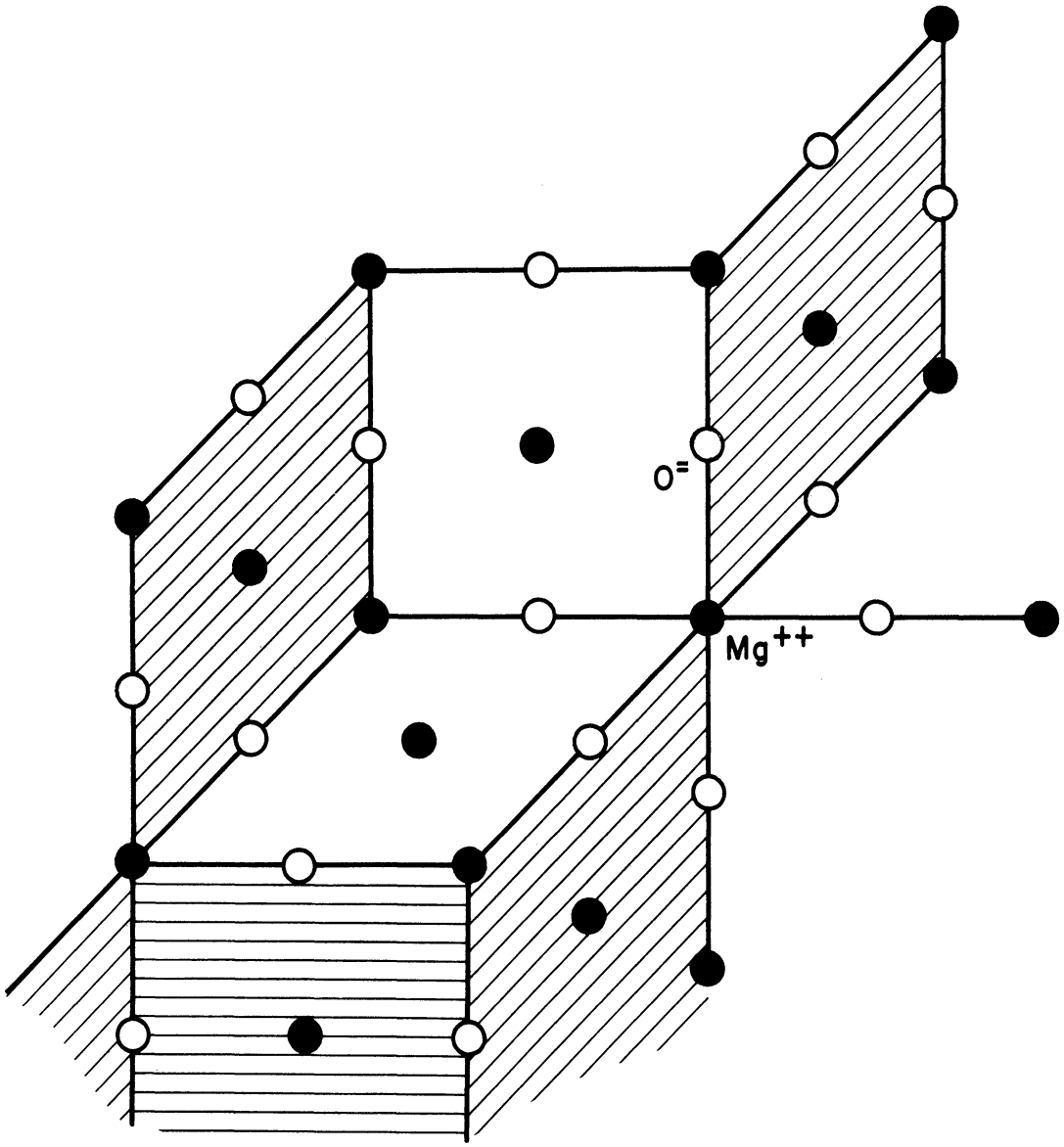

FIG. 5
Mg IN OCTAHEDRAL SYMMETRY

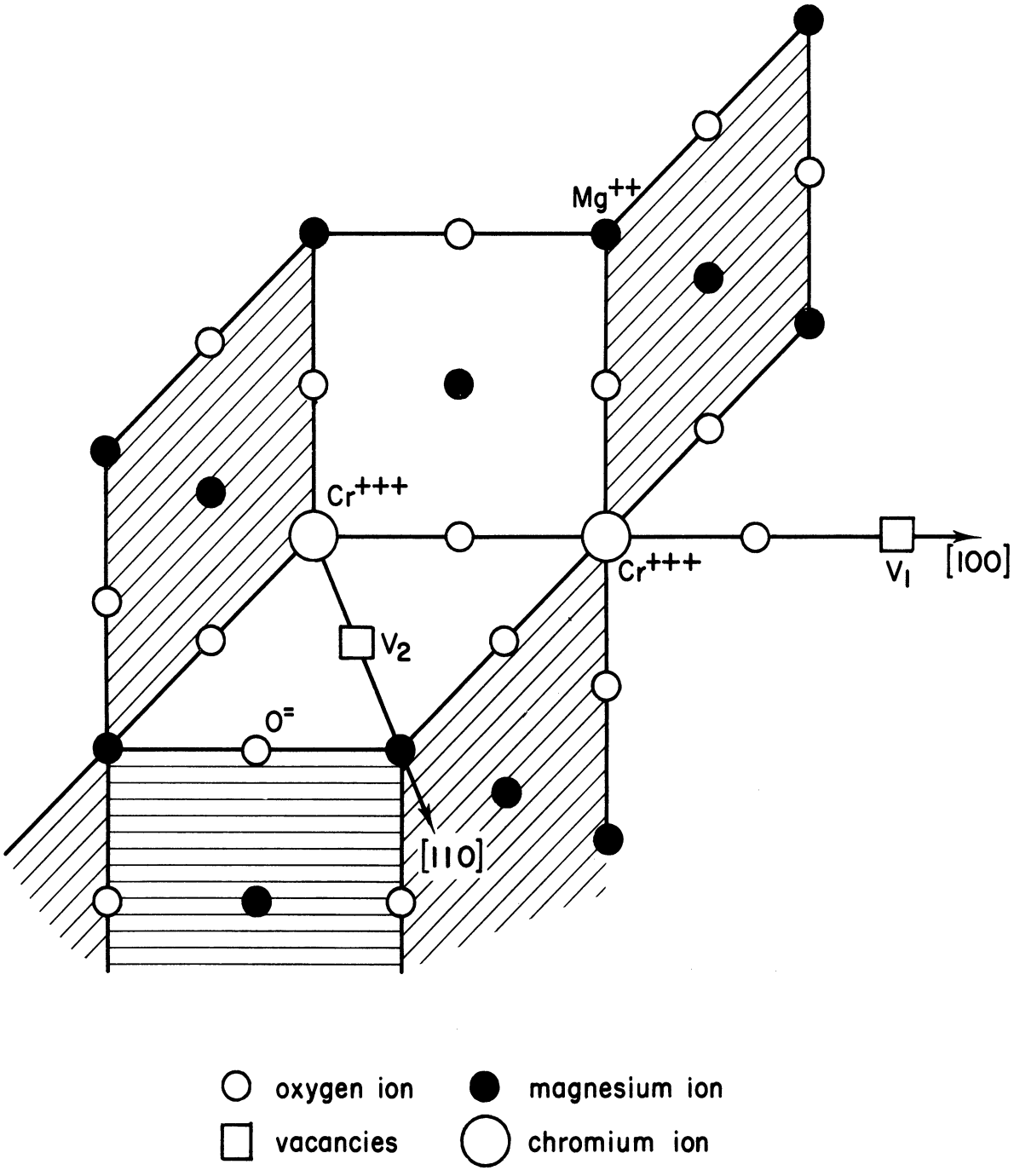

FIG 6
TWO TYPES OF Mg^{++} VACANCIES
OF AXIAL SYMMETRY

and (3) may be thought of as due to the Mg^{++} vacancies in sites V_1 and V_2 respectively, in Figure 6.

The lines arising from symmetries (1) and (2) are well identified in the paper by Wertz and Auzins[11]. As an illustration of use of the Spin Hamiltonian, we shall calculate the number and position of lines due to cubic and axial fields.

I-1. Chromium in Cubic Environment

The Cr^{+3} ion has an electron configuration of argon configuration $+3d^3$. According to Hunds' rule the ground state of this configuration is a ^4F state. Furthermore, group theoretical considerations show that the sevenfold orbital degeneracy will be removed in the cubic field, and the term splits into a singlet and two triplets with the singlet lying lowest. Thus the ground state responsible for the paramagnetic resonance absorption acts like a ^4S state with an effective spin $S' = 3/2$ in the Spin Hamiltonian. The next highest triplet is separated by about 10^4 cm^{-1} so that the spin-orbit coupling does not remove the fourfold spin degeneracy of the ground state. However, the application of magnetic field will split this ground state into four equally spaced levels (see Figure 7). This can be seen as follows. For crystalline electric field of cubic symmetry, the most general form of the Spin Hamiltonian, when $S = 3/2$, is given by

$$\mathcal{H} = \beta \underline{H} \cdot \underline{\underline{g}} \cdot \underline{S} + \underline{I} \cdot \underline{\underline{A}} \cdot \underline{S} - g_N \beta_N \underline{H} \cdot \underline{I} \ .$$

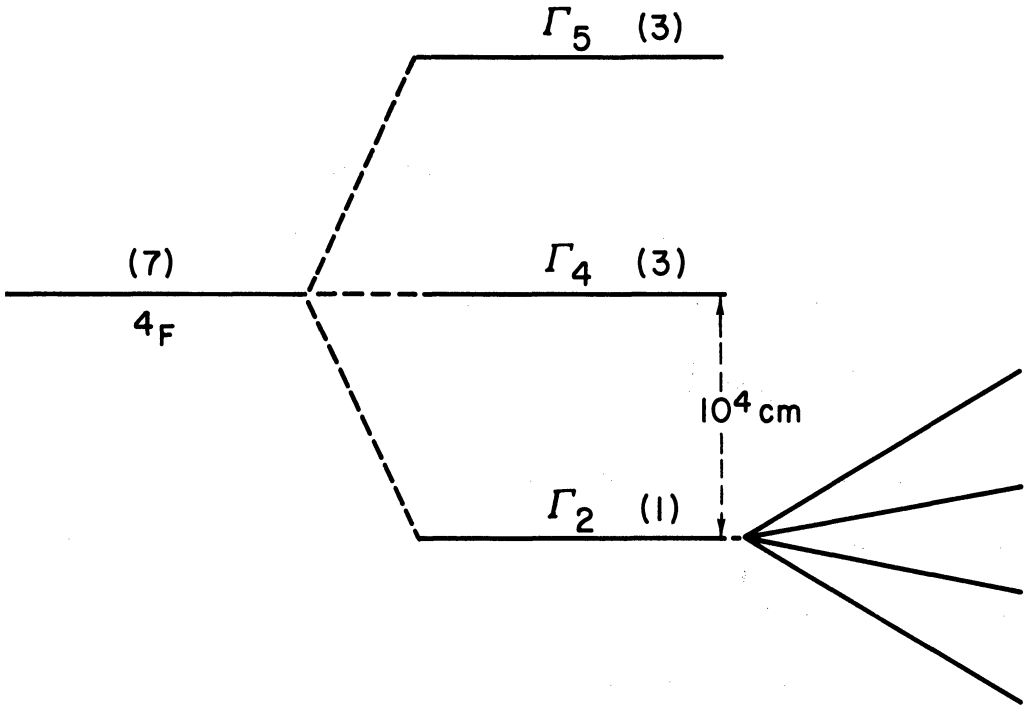
Γ_5 (3)
(7)
^4F
Γ_4 (3)
10^4 cm
Γ_2 (1)
FREE ION
CUBIC FIELD
H-FIELD

FIG 7

For our discussions, we shall assume that the tensors g and A are both isotropic. Furthermore, since the nuclear spin $I = 0$ for the isotopes Cr-50, -52, and -54, the Spin Hamiltonian for the even isotopes of chromium is just

$$\mathcal{H} = g\beta \underline{H} \cdot \underline{S}$$

so that

$$E(M) = g\beta HM$$

for $\underline{H}$ parallel to the Z-axis. The allowed transitions are the ones for which $\Delta M = \pm 1$, so that the absorption due to the isotopes Cr-50, -52, and -54 is a single line at

$$h\nu = g\beta H .$$

Experimentally, a strong line at 3338 gauss is seen for $\nu = 9.250$ KMC. This corresponds to g = 1.9797. Upon closer inspection, four weak lines spaced about 18 gauss apart flank the central line. These can be assigned to Cr-53, whose isotopic abundance is 9.5%. Its nuclear spin is 3/2, so that the terms involving the nuclear spin need to be taken into account. For the transitions $\Delta M = \pm 1$ and $\Delta m = 0$ we obtain

$$h\nu = g\beta H + Am$$

to the first order approximation. Here, I = 3/2, so m can have values 3/2, 1/2, -1/2, -3/2. Therefore, instead of one strong central line, we observe four lines with one-fortieth intensity, equally spaced with spacing $\frac{A}{g\beta}$ = 17.85 gauss (see Figure 8).

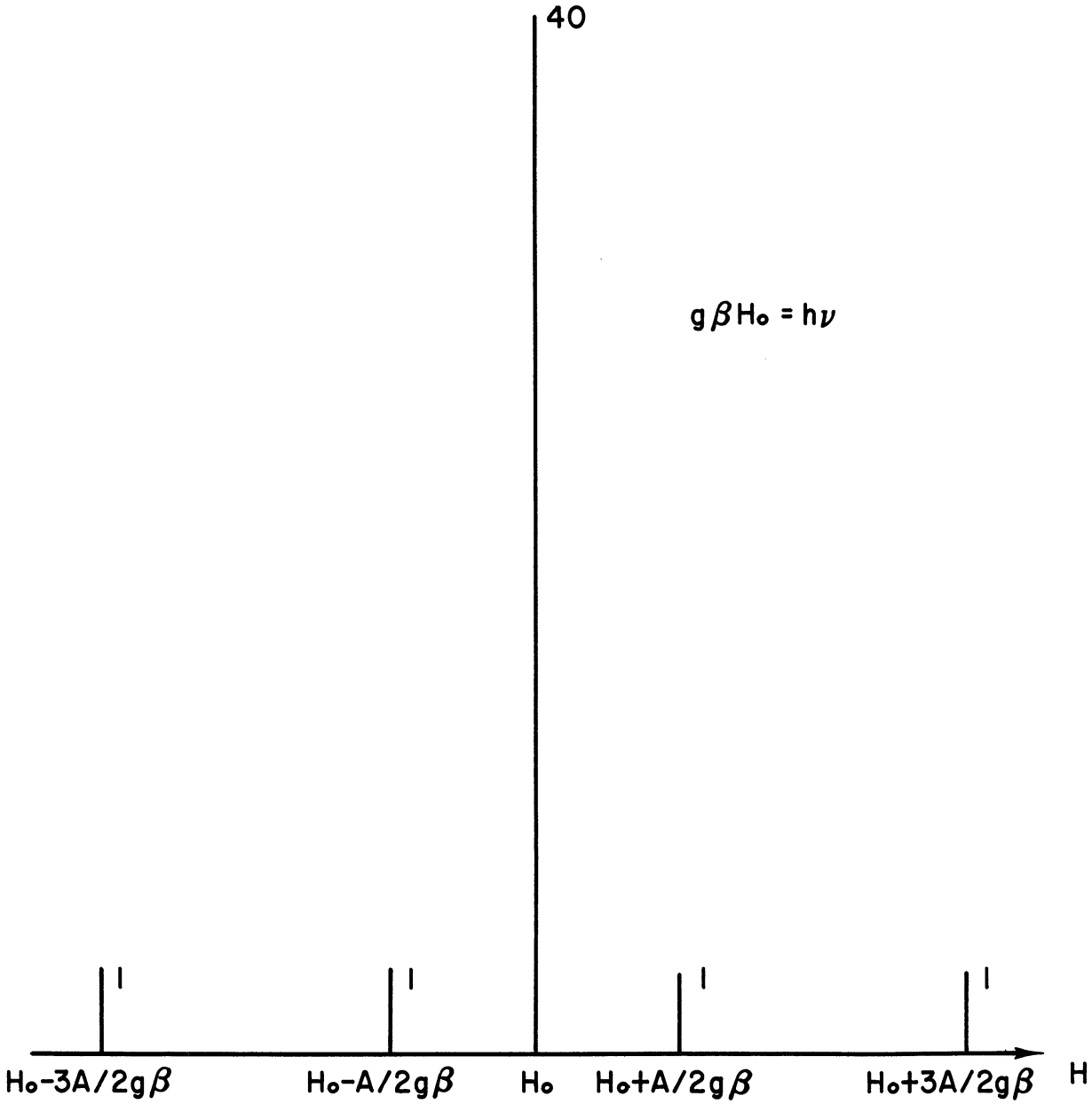
40
$g\beta H_o = h\nu$
1
1
1
1
$H_o-3A/2g\beta$
$H_o-A/2g\beta$
H_o
$H_o+A/2g\beta$
$H_o+3A/2g\beta$
H

FIG 8

I-2. Chromium in Axial Environment (Cr^{+++} associated with Mg^{++} vacancy or type V_1)

As was seen in the last section, the characteristic spectrum of Cr^{3+} in a cubic field consists of a group of isotropic lines, a strong one due to the even isotopes and four weak ones due to Cr^{53}. On the other hand, if the Cr^{3+} ion is paired with a vacancy so that the crystalline environment is lower than cubic symmetry, the absorption spectrum will no longer be isotropic. For the even chromium isotopes paired with a vacancy along the Z-axis, the appropriate Hamiltonian is given by

$$\mathcal{H}_1 = g\beta \underline{S}\cdot\underline{H} + D\left[S_z^2 - \frac{S(S+1)}{3}\right]$$

which is obtained by adding an axial term $D\left[S_z^2 - \frac{S(S+1)}{3}\right]$ to the one for cubic field but neglecting the terms involving nuclear interactions. On the other hand, with vacancies along the X- and Y-axes, the Spin Hamiltonians are given by

$$\mathcal{H}_2 = g\beta \underline{S}\cdot\underline{H} + D\left[S_x^2 - \frac{S(S+1)}{3}\right]$$

or

$$= g\beta \underline{S}\cdot\underline{H} + D\left[S_y^2 - \frac{S(S+1)}{3}\right].$$

The spectra due to these defects when the magnetic field H is along the Z-axis can be calculated as follows:

(i) Z-type

From Hamiltonian H_1

$$\mathcal{H}_1 = g\beta H S_z + D\left(S_z^2 - \frac{5}{4}\right) \; ; \; S = \frac{3}{2}$$

$$E_1(M) = g\beta H M + D\left(M^2 - \frac{5}{4}\right)$$

$$E\left(\frac{3}{2}\right) = g\beta H\left(\frac{3}{2}\right) + D = g\beta\left(\frac{3}{2}H + D'\right)$$

$$E\left(\frac{1}{2}\right) = g\beta H\left(\frac{1}{2}\right) - D = g\beta\left(\frac{1}{2}H - D'\right) \quad ; \quad D' = \frac{D}{g\beta}$$

$$E\left(-\frac{1}{2}\right) = g\beta H\left(-\frac{1}{2}\right) - D = g\beta\left(-\frac{1}{2}H - D'\right)$$

$$E\left(-\frac{3}{2}\right) = g\beta H\left(-\frac{3}{2}\right) + D = g\beta\left(-\frac{3}{2}H + D'\right)$$

with $\Delta M = \pm 1$, we get three lines (see Figure 9)

$$h\nu = g\beta(H_1 + 2D') \longrightarrow H_1 = \frac{h\nu}{g\beta} - 2D'$$

$$h\nu = g\beta(H_2 + 0) \longrightarrow H_2 = \frac{h\nu}{g\beta}$$

$$h\nu = g\beta(H_3 - 2D') \longrightarrow H_3 = \frac{h\nu}{g\beta} + 2D'$$

The three lines were actually found at

H_1=1555, H_2=3330, H_3=5105 gauss

therefore,

$4D' = H_3 - H_1 = 5105 - 1555 = 3550$ gauss

so $D' = 887$ gauss.

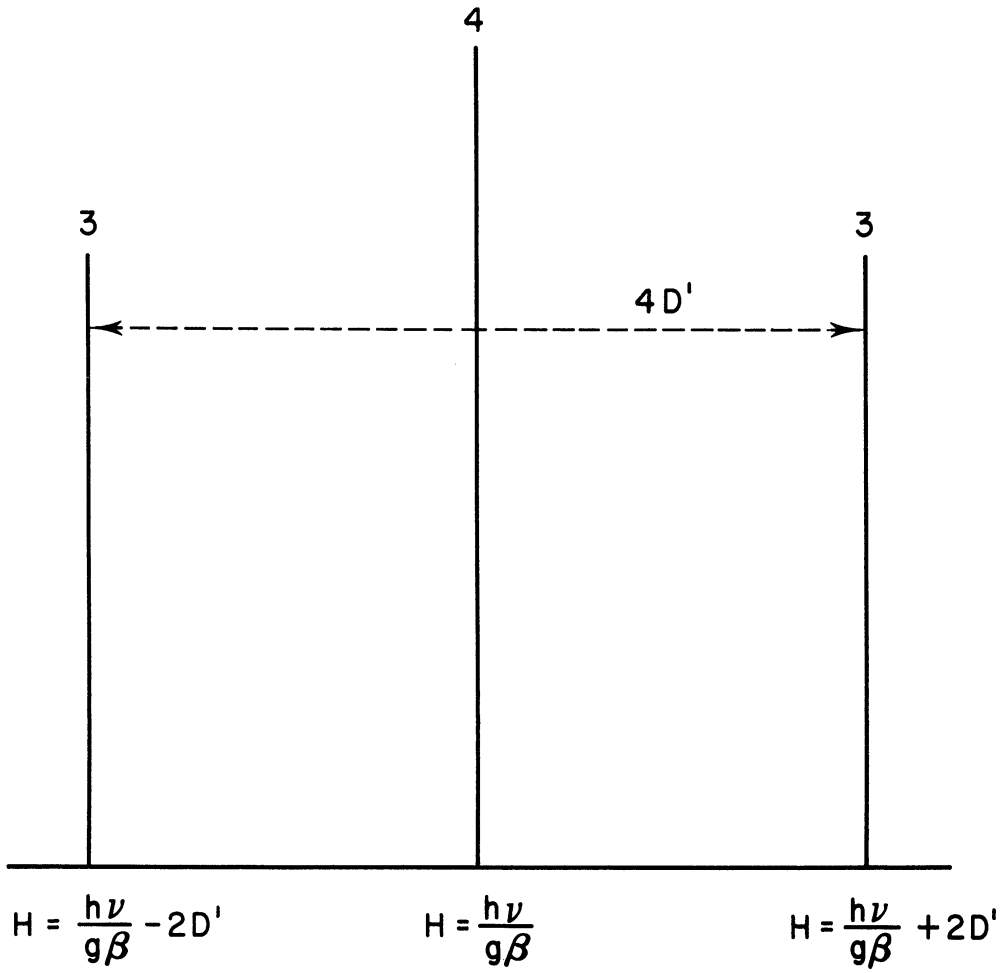

FIG 9

The g-value can be found from

$$H_1 + H_3 = \frac{2h\nu}{g\beta} = 6650 \text{ gauss}$$

$$g = \frac{2h\nu}{6650\beta} = 1.9782$$

The intensity of the lines M $\longrightarrow$ M - 1 is proportional to

$|S(S + 1) - M(M - 1)|$,

M = 3/2: $\quad 15/4 - 3/4 = 3$

M = 1/2: $\quad 15/4 + 1/2 = 4$

(ii) X (or Y) - type

From Hamiltonian (2) $\mathcal{H}_2 = g\beta HS_z + D\left[S_x^2 - \frac{S(S+1)}{3}\right]$

$$\mathcal{H}_2 = g\beta HS_z + D\left[\left(\frac{S_+ + S_-}{2}\right)^2 - \frac{5}{4}\right]$$

$$= g\beta HS_z + D\left[\frac{1}{4}(S_+^2 + S_-^2) + \frac{1}{4}(S_+S_- + S_-S_+) - \frac{5}{4}\right]$$

use the identity

$$S^2 = S_z^2 + \frac{1}{2}(S_+S_- + S_-S_+)$$

$$\frac{1}{4}(S_+S_- + S_-S_+) = \frac{1}{2}\left[S(S+1) - S_z^2\right]$$

$$= \frac{1}{2}\left[\frac{15}{4} - S_z^2\right]$$

Hence

$$\mathcal{H}_2 = g\beta HS_z - \frac{D}{2}\left(S_z^2 - \frac{5}{4}\right) + \frac{D}{4}(S_+^2 + S_-^2)$$

From the secular determinant (see Figure 10) we get two secular equations

(1) $$\left(\frac{D}{2}+\frac{1}{2}g\beta H-E\right)\left(-\frac{D}{2}-\frac{3}{2}g\beta H-E\right)=\frac{3}{4}D^2$$

(2) $$\left(\frac{D}{2}-\frac{1}{2}g\beta H-E\right)\left(-\frac{D}{2}+\frac{3}{2}g\beta H-E\right)=\frac{3}{4}D^2$$

Then, from (1) we get

$$E=D\left[-\frac{x}{2}\pm\sqrt{1+x+x^2}\right] \; ; \quad x=\frac{g\beta H}{D}$$

Similarly from (2), we get

$$E=D\left[\frac{x}{2}\pm\sqrt{1-x+x^2}\right]$$

Therefore, we have four energy levels

$$E_1 = D\left(\frac{x}{2}+\sqrt{1-x+x^2}\right)$$

$$E_2 = D\left(-\frac{x}{2}+\sqrt{1+x+x^2}\right)$$

$$E_3 = D\left(\frac{x}{2}-\sqrt{1-x+x^2}\right)$$

$$E_4 = D\left(-\frac{x}{2}-\sqrt{1+x+x^2}\right)$$

from which we get three unequally spaced lines. It is easily shown that the Hamiltonian of the Y-type

$$\mathcal{H}=g\beta HS_z+D\left(S_y^2-\frac{S}{3}(S+1)\right)$$

gives exactly the same four energy levels. Therefore, X-type and Y-type lines coincide. This is also evident from the symmetry considerations.

	$-\frac{3}{2}$	$-\frac{1}{2}$	$\frac{1}{2}$	$\frac{3}{2}$
$-\frac{3}{2}$	$-\frac{D}{2}-\frac{3}{2}g\beta H$ $-E$	0	$\frac{\sqrt{3}}{2}D$	0
$-\frac{1}{2}$	0	$\frac{D}{2}-\frac{1}{2}g\beta H$ $-E$	0	$\frac{\sqrt{3}}{2}D$
$\frac{1}{2}$	$\frac{\sqrt{3}}{2}D$	0	$\frac{D}{2}+\frac{1}{2}g\beta H$ $-E$	0
$\frac{3}{2}$	0	$\frac{\sqrt{3}}{2}D$	0	$-\frac{D}{2}+\frac{3}{2}g\beta H$ $-E$

FIG 10

In the actual experiment, these lines are found at

$$H_1' = 2480, \quad H_2' = 3145, \quad H_3' = 4200 \text{ gauss}$$

In the set-up that H $\parallel$ Z-axis, the microwave field H_m is, say $\parallel$ to X-axis (see Figure 11). Then, by 90^o rotation of the sample (x → x, y → z, z → y) around this microwave field, one can actually observe that the lines H_1, H_2, and H_3 will respectively interchange places with one each of H_1', H_2', and H_3' lines. This angular variation of the positions of lines can also assure the crystalline field is axial.

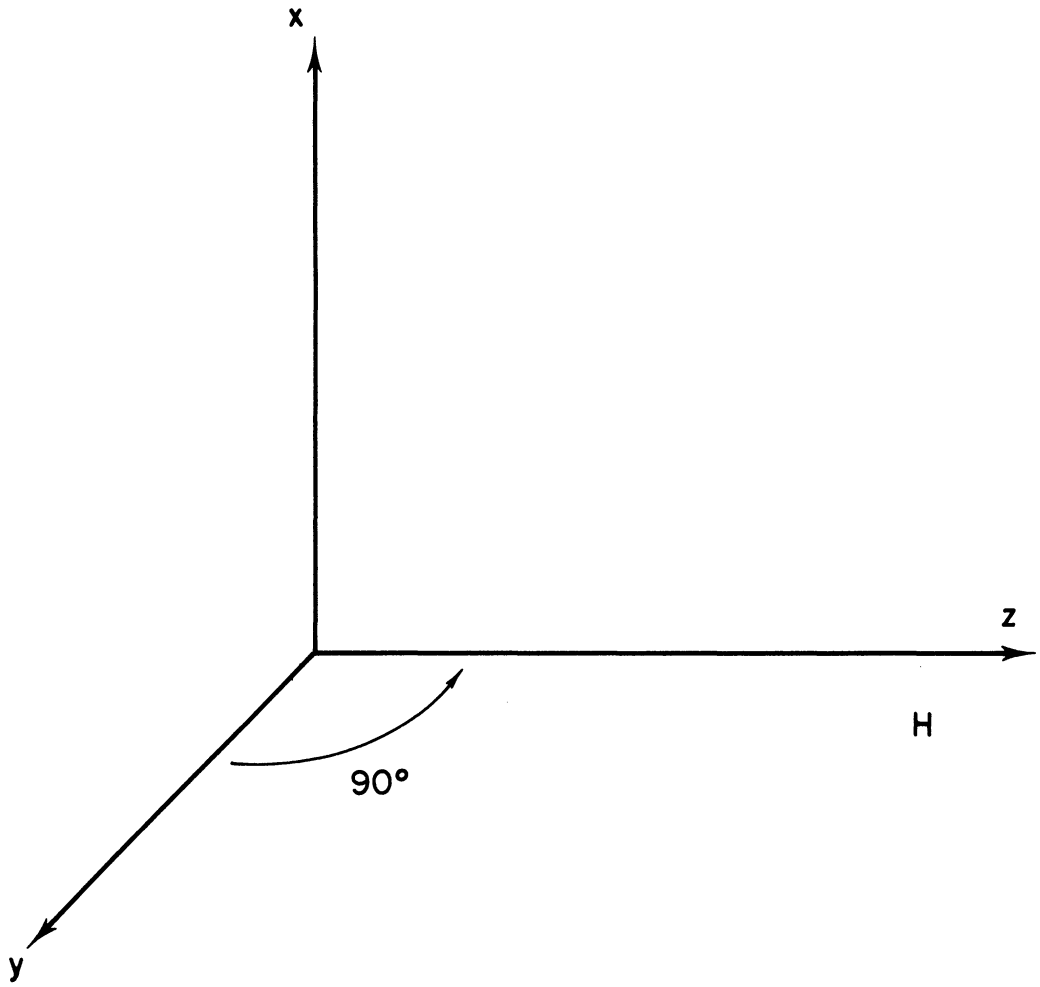

FIG 11

II. Oxygen Vacancies Produced by Neutron Irradiation

We shall show next how defects produced by MgO by neutron irradiation are $O^{=}$ vacancies with trapped electrons. The motivation for the search of F-centers in MgO stems from the studies of F-centers in alkali halides. In 1949, C. A. Hutchison[12] observed the paramagnetic absorption spectrum of F-centers in LiF produced by neutron irradiation. Later, the theoretical interpretation of the results was provided by Kittel and his students[13], and the correctness of the interpretation has been established beyond doubt by the so-called ENDOR technique developed by G. Feher[14, 15].

An F-center, according to the presently accepted model, is a negative ion vacancy with trapped electrons. These electrons have some unusual properties because they do not experience central attractive forces as do electrons associated with a definite nucleus. Because of the absence of a central attractive force, the electron tends to spend much of its time in the periphery of the vacancy, and in particular, the electron charge density near and at the surrounding positive ions is quite appreciable.

II-1 Number of $O^{=}$ Vacancies

MgO crystals were subjected to neutron irradiation ranging from 1 to 3 x 10^{19} (nvt); the resultant F-center ESR spectra showed that 1.4 x 10^{19} cm^{-3} F-centers were produced, corresponding to one F-center produced for every 5.7 incident neutrons. The concentration 1.4 x 10^{19} cm^{-3} was obtained by comparing the

area under the integral asorption curve of the irradiated sample with another sample containing a known concentration of paramagnetic free radicals.

II-2 Identification of Center

For even isotopes Mg^{24} and Mg^{26} (total abundance 89.9%) I = 0. Therefore in the Spin Hamiltonian, there is only the one Zeeman term, i.e.

$$H = g\beta \underline{H} \cdot \underline{S}$$

giving the strong line at $h\nu = g\beta H$

The observed H corresponds to g = 2.0023 $\pm$ o.0001, nearly equal to that of free electron value. This indicates that the signal is from an electron trapped in $O^{=}$ vacancy. The other evidence is the existence of hyperfine multiplets. Since the 10.11% Mg^{25} isotope has a non-vanishing nuclear moment, (I = 5/2, as a consequence of observation of six hyperfine components), one should expect to see hyperfine structures.

Among all Mg^{++} octahedra, some should contain one or two Mg^{++} ions. From isotopic abundance data, it is not difficult to show that there are octahedra

(i) of only Mg^{24} and Mg^{26}.....53%

(ii) having one Mg^{25}.....36%

(iii) having two Mg^{25}.....10%

A center with one Mg^{25} in the octahedron can be described by the following Spin Hamiltonian (only the nuclear-electron interaction part)[16],

$$\mathcal{H} = g\beta \underline{H}\cdot\underline{S} + a\underline{I}\cdot\underline{S} + \frac{b}{2}(3\cos^2\theta - 1)(3I_z S_z - \underline{I}\cdot\underline{S}),$$

where the second and third term represent isotropic and anisotropic magnetic interaction of an F-center electron with the Mg^{25} nucleus, and z-axis is taken to be the axis of symmetry.

Further

$$a = \frac{16\pi\beta\mu}{3I}\left|\psi(Mg^{25})\right|^2$$

$$b = \frac{\beta\mu}{I}\left\langle \frac{3\cos^2\theta_F - 1}{r_F^3} \right\rangle \qquad (\mu: \text{ nuclear moment of } Mg^{25})$$

and r_F: position vector of the F-center electron measured from the Mg^{25} nucleus as the origin.

θ_F: angle between electron position vector r_F and the symmetry axis.

Now if a strong magnetic field $\underline{H}$ is applied making angle θ with the symmetry axis, then we can take the direction of the field as the axis of quantization. Thus, to the first order perturbation approximation

$$E(M,m) = g\beta HM + amM + b(3\cos^2\theta - 1)mM$$

In ESR absorption, we have $\Delta M = \pm 1$, $\Delta m = 0$

$$h\nu = g\beta H + [a + b(3\cos^2\theta - 1)]m .$$

Experimentally we observe six lines corresponding to I = 5/2.

The separation between each line is the same and is equal to

$$d = a + b(3\cos^2\theta - 1).$$

If now the applied field $\underline{H}$ is to be perpendicular to [100] direction, we will observe three sets of hyperfine sextet corresponding to one Mg^{25} nucleus located along [100], [010] and [001] axes respectively. As we rotate the sample around [100] axis

(a) Sextet due to Case (1) will remain unchanged in the position with the line separation given by

$$d = a + b(3\cos^2 90^\circ - 1) = a - b$$

(b) Sextet due to Cases (2) and (3) will change positions with the spacing between lines given by

$$d = a + b(3\cos^2\theta - 1)$$

where θ is the angle $\underline{H}$ makes with [001] and [010] directions respectively (see Figure 12).

From these observations, Wertz et. al.[17] were able to deduce

$$\frac{a}{g\beta} = 4.00 \text{ gauss}, \quad \frac{b}{g\beta} = 0.47 \text{ gauss}.$$

This angular dependence also supports the model in which an F-center is a trapped electron with one of the octahedral positions occupied by an Mg^{25} ion. The ten hyperfine components arising from two Mg^{25} ions occupying sites in the same octahedron are also found by Wertz.

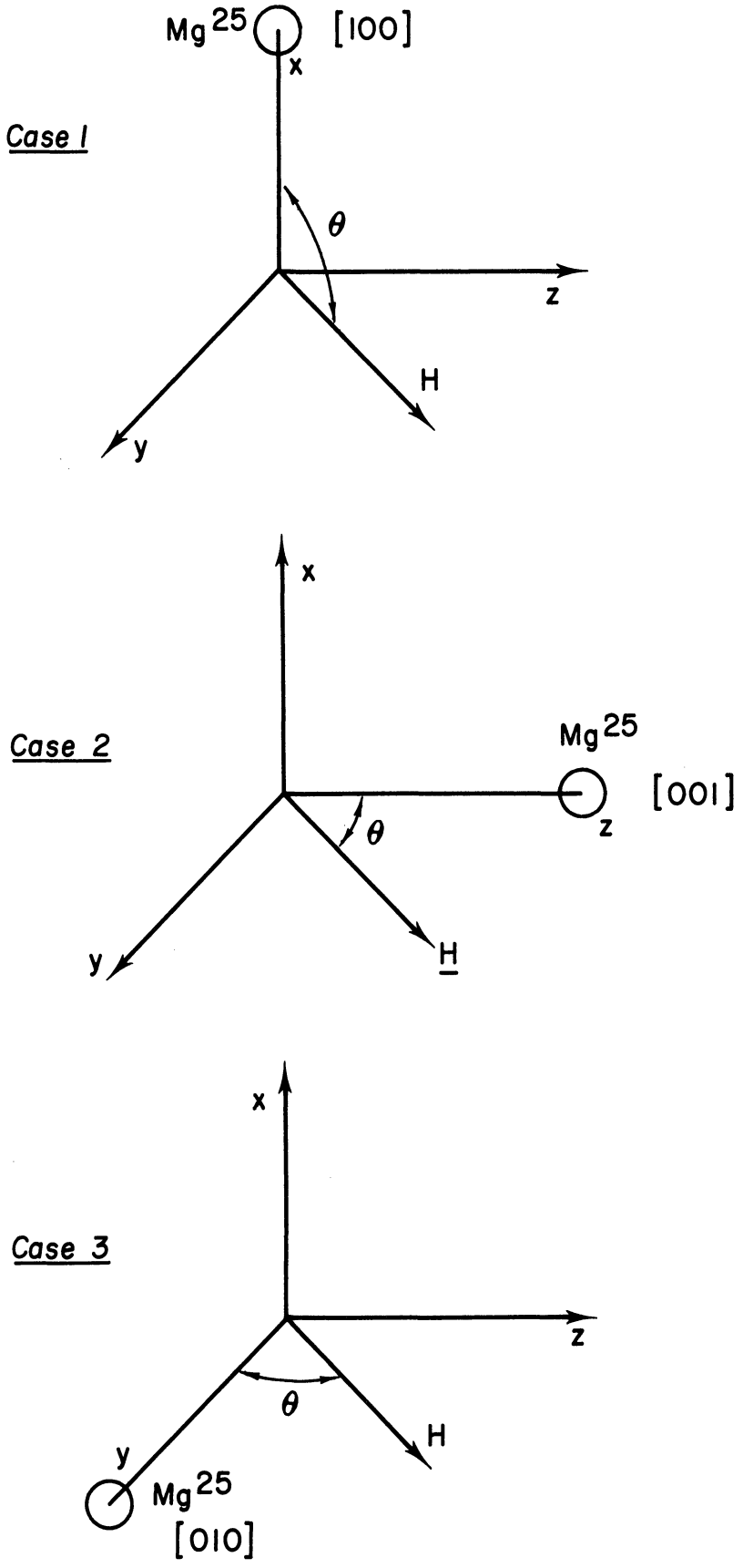
Mg25
[100]
x
Case 1
θ
z
H
y
x
Case 2
Mg25
[001]
θ
z
y
H
x
Case 3
z
θ
H
y
Mg25
[010]

FIG 12

II-3 Discussion of s-electron Wave Function

Let us see how we can use the above information to get some information about the spread of electron wave function. For this let us focus our attention on the isotropic part, which has its origin in the s-electron wave function at the Mg^{25} nucleus.

The experimental value for $a/g\beta$ = 4 gauss gives

$$a = g\beta(4.0) = 2(0.927)(4)\times 10^{-20} = 7.42\times 10^{-20} \text{ ergs}$$

But since

$$a = \frac{16\pi\beta_N\mu}{3I}|\psi(Mg^{25})|^2$$

(The wave function is evaluated at the point of nucleus.)

$$\mu_N = g_N\beta_N I = (0.3419)(5.05\times 10^{-24})\left(\frac{5}{2}\right) = 4.318\times 10^{-24} \text{ ergs/gauss}$$

$$I = \frac{5}{2}$$

Hence

$$|\psi(Mg^{25})|^2 = 0.275\times 10^{24} \text{ cm}^{-3}$$

On the other hand

$$|\psi(Mg^{++})|^2_{Free} = 17.1\times 10^{24} \text{ cm}^{-3}$$

Therefore

$$\frac{|\psi(Mg^{25})|^2}{|\psi(Mg^{++})|^2_{Free}} \simeq \frac{1}{62}.$$

From this figure we can roughly picture the length of time the center electron spends in the position of an Mg^{25} nucleus. The above figure shows that the F-center electron is quite localized in the vacancy. It spends only about 1/62 of

its time in the vicinity of the Mg^{25} nucleus in comparison to the s-electron in a free Mg^{++} ion.

III. Neutron Cross Section Measurement by Spin Resonance

This example is chosen to illustrate that several nuclear parameters can be determined by ESR. They are:

(1) Magnetic moments of Gd^{155} and Gd^{157};

(2) Isotope abundance of odd isotopes;

(3) Neutron cross sections.

III-1 Ratio of Magnetic Moment

Both Gd^{155} and Gd^{157} have I = 3/2. This was obtained by Speck[18] from optical hyperfine structure of gadolinium enriched in the isotopes Gd^{155} and Gd^{157}. Since gadolinium in ThO_2 crystal (F.C.C. structure) has a ground state of $^8S_{7/2}$, an s-state ion, the hyperfine coupling constant A is given by

$$A = \frac{16}{3}\pi g_N \beta_N \beta |\psi(0)|^2$$

where $\mu_N = g_N \beta_N I$ namely, nuclear moment $\mu_N \propto A$ for atoms with identical electronic configuration.

In Section I-2, it is shown that the spacing of each hyperfine multiplet is equal to A. Therefore, by measuring the corresponding hyperfine spacing of two Gd isotopes, Low and Shaltiel[19] obtained the ratio of its nuclear moments.

$$\frac{A(Gd^{155})}{A(Gd^{157})} = \frac{\mu_N(Gd^{155})}{\mu_N(Gd^{157})} = 0.7495 \pm 0.0045 .$$

III-2 Isotopic Abundance

For the measurement of nuclear parameters, a single crystal of ThO_2 containing less than 0.01% of natural gadolinium is used. Investigations indicate that the gadolinium atoms occupy thorium substitutional sites, surrounded by oxygen ions that produce a cubic crystalline electric field. The overall splitting of the $^8S_{7/2}$ ground state of Gd^{+++} is about 0.1755 cm^{-1}, so that at low magnetic fields, transitions corresponding to $M = \pm 3$, ± 4, and ± 5 can be observed with fairly large intensities. The line widths of these low-field transitions are found to be less than 1 gauss along the [100] crystal directions, so that the complete hfs. spectrum of the odd isotopes 155 and 157 could be obtained.

This property was used to measure the abundance and the cross section of the gadolinium isotopes.

By carefully measuring the amplitude and the integrated intensity of the two outer pairs of the hyperfine structure components of Gd^{155} and Gd^{157}, and that of the central line which corresponds to the even isotopes, Low et al.[18] were able to determine the abundance of the Gd^{155}, Gd^{157} and combined even isotopes (see Figure 13). The result is listed in the following table where it is compared with the mass spectrographic data from Collins et al.[20] (see Figure 14).

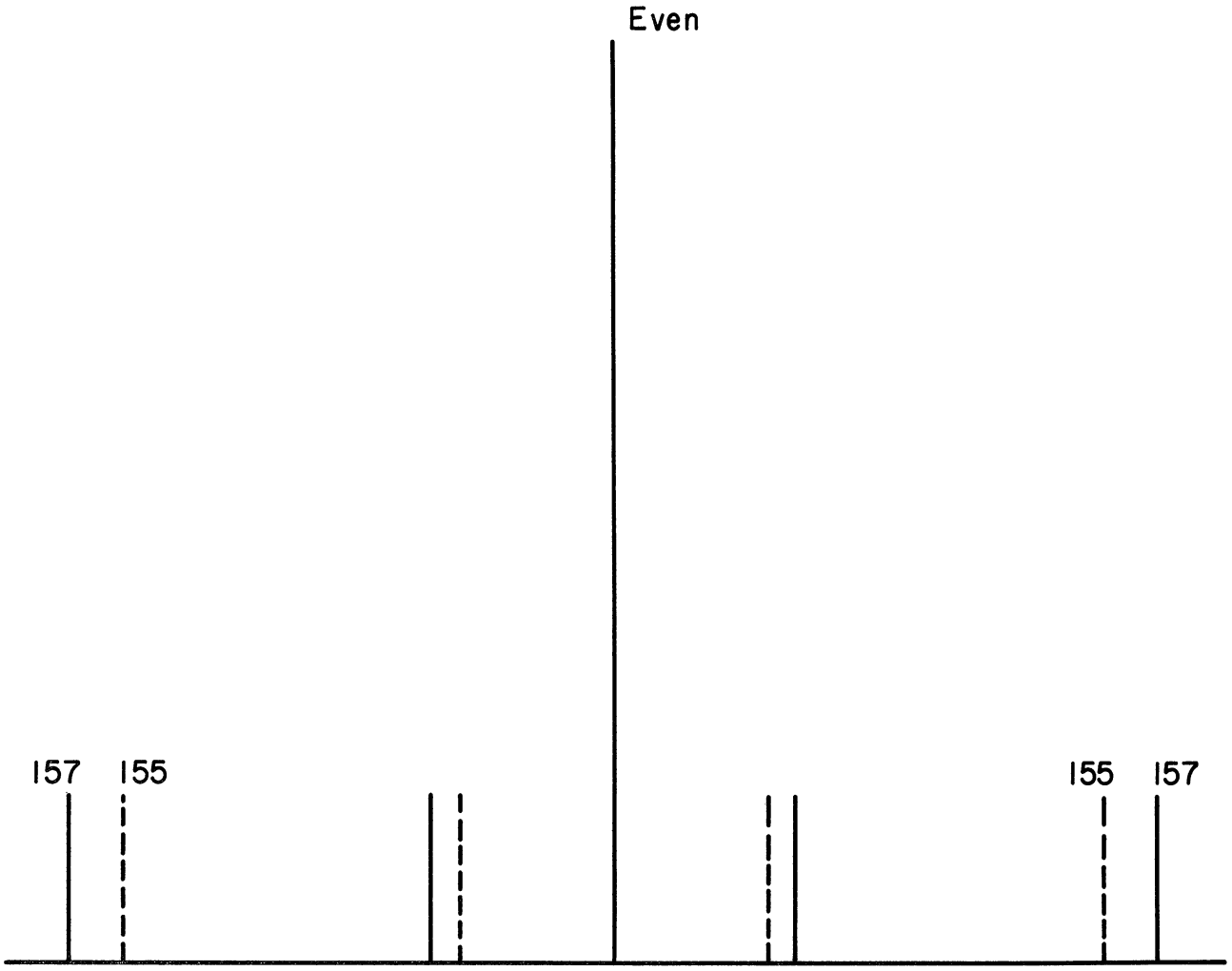

FIG 13

LINE PATTERN OF Gd IN Th_2O SINGLE CRYSTAL

	SR (Low & Shaltiel)[19]	M·S (Collins)[20]
Gd^{155}	15.05%	15.1%
Gd	15.5%	15.7%
Even isotopes	65.45%	69.2%

FIG 14

ISOTOPIC ABUNDANCE OF NATURAL Gd
MEASURED BY SPIN RESONANCE TECHNIQUE AND MASS SPECTROGRAPH

III-3 Neutron Capture Cross Section

It has been pointed out that the large neutron capture cross section of Gd is due to the odd isotopes, i.e. Gd^{155} and Gd^{157}. Furthermore, the cross sections of isotope 155 and 157 are also expected to be quite different. Therefore, by neutron irradiation of the sample (ThO_2) containing natural Gd, and then by the measurement of the isotopic abundance of 155 and 157, one should be able to find out the ratio of their neutron capture cross sections. In doing this, the following assumptions must be made:

(1) The neutron cross section of the even isotopes is negligible. (Experimental evidence seems to indicate that the even isotopes contribute at most about 1000b, to the total cross section of 46,000b.)

(2) The fission products of Th contribute a negligible amount to the Gd present in the sample.

(3) The neutron bombardment does not remove preferentially various Gd isotopes from the cubic lattice sites.

(4) The α, β and γ radiation do not cause transmutation of Gd isotopes.

The abundance of Gd^{155} and Gd^{157} was measured before and after four weeks of bombardment in the Harwell pile (Thermal flux: 5×10^8 n/cm^2, Fast flux: 9×10^{17}n/cm , sample size: 0.3 cm^3), the result was:

	Before	After
Gd^{155}	15.05 ± 0.2%	12.7 ± 0.25%
Gd^{157}	15.5 ± 0.2%	10.4 ± 0.3 %

Since the sample is small (0.3 cm^3), the law of depletion for Gd^{155} and Gd^{157} is given by

$$-\frac{dN}{dt} = \sigma \phi N$$

where ϕ = neutron flux

σ = neutron cross section of either Gd^{155} or Gd^{157}

N = concentration of either Gd^{155} or Gd^{157} in no. of atoms/cm^3 in the sample.

Then

$$\phi t \sigma^{155} = \ln \frac{N^{155}(0)}{N^{155}(t)}$$

$$\phi t \sigma^{157} = \ln \frac{N^{157}(0)}{N^{155}(t)}$$

so that

$$\frac{\sigma^{157}}{\sigma^{155}} = \frac{\ln [N^{157}(0)/N^{157}(t)]}{\ln [N^{155}(0)/N^{155}(t)]} = \frac{\ln (15.5/10.4)}{\ln (15.0/12.7)} = 2.35$$

Using σ(Gd) = 46,000 ± 2000 barns

Low et al. got σ(157) = 210,000b.

σ(155) = 88,700 b.

in comparison with Collins[20] et al. and Hughes[21] value

Collins et al.[20]	Hughes[21]
σ(157) = 209,000 b.	160,000 ± 60,000 b.
σ(155) = 87,200 b.	70,000 ± 20,000 b.

Whereas a direct measurement by Jowith et al.[22] gives

$\sigma(157) = 238{,}500 \pm 2000$ b.

$\sigma(155) = 55{,}800 \pm 600$ b.

IV Nuclear Spins, Magnetic Dipole Moments, and Electric Quadrupole Moments of Certain Iron Group Nuclides

From the foregoing discussions, it is clear that the electron spin resonance is an important tool for the measurement of nuclear spins and moments. The phenomenon of hyperfine structure in solids was discovered first by Penrose and by Ingram[23]. The systematic investigations of this effect, and the subsequent measurement of spins and moments of odd-proton-odd-neutron nuclides, were made by B. Bleaney[24] and his collaborators at Oxford. Many of the initial measurements served to confirm earlier optical hfs. measurements or to remove the uncertainties of the experimental results. We shall not discuss these measurements. Rather we shall focus our attention on those nuclides whose nuclear parameters would be difficult to measure by optical techniques, again to emphasize the power of the ESR method. We shall first discuss the nuclear spin and magnetic moment measurements, and consider a new technique that is currently being developed to measure the electric quadrupole moments of nuclei.

A. Nuclear Spins and Magnetic Dipole Moments

1. Odd-Odd Nuclei.

The following table summarizes the results obtained by the ESR method:

Nuclide	$T_{1/2}$	I (Exp)	Proton Shell	Neutron Shell
$_{23}V^{50}$	4×10^{14} yr (.25% abundant)	6	7/2	7/2(Co^{59})
$_{25}Mn^{56}$	2.58 hr	3	5/2	1/2(Fe^{57})
$_{27}Co^{56}$	77.3d	4	7/2	3/2(Cr^{53})
$_{27}Co^{58}$	71.3d	1 or 2	7/2	1/2(Fe^{57})
$_{27}Co^{60}$	5.24y	5	7/2	3/2(Cr^{53})

In the last three columns, the experimentally observed values of the spins, the odd proton and odd neutron shells are indicated. For example, for Mn^{56}, the 25 proton shell of Mn^{55} has spin 5/2, and the 31 neutron shell of Fe^{57} has spin 1/2. We observe that the nuclear spins of these nuclides are the sums or 1 less than the sum, of the spins of the odd nuclear shells. This is a part of a rule first enunciated by Nordheim[25]. The exception is Co^{58}, for which the spin is closer to the difference of the spins of the proton and neutron shells.

The ratio of the magnetic moment to that of the stable isotope can be obtained by taking the ratio of the hfs. coupling constant A. For example, Kikuchi[26], Sivertz, and Cohen measured the hfs. splittings of V^{51} and V^{50} and obtained the value

$$\frac{A\ (V^{50})}{A\ (V^{51})} = 0.3792 \pm 0.0008$$

Strictly speaking, this value is not the ratio of the magnetic moments, because the hfs. coupling constant depends also upon the value of the wave function within the nucleus. The ratio of the nuclear magnetic moments has been obtained by Walchli

and Morgan[27] to be

$$\frac{g_N(V^{50})}{g_N(V^{51})} = 0.379074 \pm 0.000017 .$$

It may be of interest to re-measure the parameter A and g_N to determine the hfs. anomaly.

2. Odd Neutron Nuclei

Nuclide	Abundance	I	μ_N
Cr^{53}	9.55%	3/2	-0.4735
Fe^{57}	2.17%	1/2	+0.0903
Ni^{61}	1.25%	3/2	0.30

3. Odd Proton Nuclei (Radioactive)

Nuclide	T 1/2	I	μ_N
V^{49}	330	7/2	= 4.46
Mn^{53}	2×10^6	7/2	= 5.050
Co^{57}	270	7/2	= 4.65

4. Nuclei of Non-paramagnetic Ions

In the examples discussed so far, the electron-nuclear interactions were brought about by the unpaired electrons of the paramagnetic ions. We shall discuss here the magnetic moment determination of Au^{197}, which is normally non-paramagnetic, but which exhibits hfs. when paired with a chromium in the silicon lattice. From the standpoint of solid-state physics, this method is of interest because it shows how the Cr and Au impurities are

paired.

When Cr and Au are both introduced into Si by diffusion at about 1300°C, observations indicate that the following processes take place: the Au finds substitutional sites in the lattice, while Cr remains in interstitial sites at the diffusion temperatures. As the sample is cooled, the Cr atoms move into interstitial positions adjacent to, and in, the [111] directions from the substitutional Au atoms and form the Au-Cr pairs.

The experimental observations are consistent with the (Cr-Au) pair being neutral and having a total electron spin of 3/2. The axial field arising from the pairing can be described by the DS_Z^2 in the Spin-Hamiltonian, with D = 6.7 cm^{-1}. By means of double resonance experiments, Woodbury and Ludwig[45] found

$$g_N(Au^{197}) = +0.0959 \pm 0.0003$$

with $I = 3/2$

$$\mu_N(Au^{197}) = g_N \beta_N I = +0.1437 \pm 0.0004 \text{ nm}.$$

in agreement with the atomic beam value of

$$\mu_N(Au^{197}) = +0.1431 \pm 0.0014 \text{ nm}.$$

reported by Fricke, Penselin and Rechnagel[28].

5. Nuclear Moments of Ni^{61} and Fe^{57}

The importance of the ESR technique to nuclear physics stems from the fact that it is possible to make measurements of spins

and moments of nuclei having low abundance and small nuclear magnetic moments. Examples of these are Ni^{61} (1.25%) and Fe^{57} (2.17%), both of which are odd neutron nuclei. The nucleus Ni^{61} will be discussed first, in order to emphasize the need of future precision measurement, and then Fe^{57}, in order to show how absolute measurements of nuclear moments can be made by the ENDOR technique. Of course, as is well known, the last nucleus is important in the Mossbauer effect.

The nuclear spin of Ni^{61} was shown to be 3/2 by Woodbury and Ludwig[29] from the ESR spectrum of Ni-doped germanium. Samples were prepared by plating 5 to 10 mg of Ni enriched in Ni 61 to about 83% onto an arsenic-doped germanium crystal of dimensions 3 x 3 x 12 mm^3. The nickel was then diffused into germanium by heating to 850°C for seventy-five minutes. The Ni atoms were then in Ni^- state (with $S' = \frac{1}{2}$). The arsenic atoms were introduced to control the concentration of Ni^-. The maximum concentration of Ni in the crystal was 7×10^{15} Ni/cm^3. Since the $S' = \frac{1}{2}$, there was only one resonant transition ($M=-\frac{1}{2} \rightarrow M = \frac{1}{2}$) for each N^- site, with accompanying 4 hf equal intensity lines (at T = 21°K), indicating the I = 3/2, and the separation between adjacent components is found to be 10.5 gauss.

Since no other isotope of known magnetic moment is available, it is not possible to determine the Ni^{61} magnetic moment from the hfs. coupling constant. However, Orton, Auzins, and Wertz[30] have indicated how an estimate of the magnetic moment can be made.

These investigators succeeded in detecting the ESR spectrum of Ni^{61} in unenriched nickel occurring as an impurity (Ni^{+2}) in MgO. The hfs. coupling constant was found to be

$$A(Ni^{61}) = (8.3 \pm 0.4) \times 10^{-4} \text{ cm}^{-1}$$

which is comparable to the value found in germanium.

To obtain an estimate of the magnetic moment, the above hfs. coupling constant was compared to that of Co^{+1} which is isoelectronic with Ni^{++} ($3d^8$). The spectrum of Co^{+} in MgO was observed at 77°K, following x-irradiation of sample containing Co^{++}. The spectrum of Co^{++} is characterized by g = 4.278 and A = 97.8 x 10^{-4} cm^{-1}. For Co^{+}, on the other hand, g = 2.1728 and A (Co^{59}) = (54.0 = 0.2) x $10^{-4}{}_{cm}{}^{-1}$. Now both Ni^{++} and Co^{+}free ions have a ground term of ^3F and under the perturbation of cubic crystalline field, this ^3F term splits into three levels with the orbital singlet level $^3F_2$ lying lowest[39]. In this orbital singlet ground state, if one carried out the usual non-degenerate perturbation calculation for the electron-nuclear magnetic interaction, one can show[6] that to the first order, the hyperfine coupling constant A is approximately zero. However, due to the configurational interaction, a small amount of configuration $3s3p^6 3d^8 4s$ might be admixed into the original configuration $3s^2 3p^6 3d^8$. The existence of unpaired s-electrons in the admixed configuration then can contribute through the Fermi contact term to the hyperfine coupling constant A, which is given by[6]

$$A = -\frac{2\beta\beta_N \mu_N}{I}\langle r^{-3}\rangle K$$

where $\langle r^{-3}\rangle$ is the average over the radial part of the 3-**d** orbital and **K** is the measure of degree of admixed configuration $3s3p^6 3d^8 4s$.

Abragam, Horowitz and Pryce[46] found that the product $\langle r^{-3}\rangle K$ is approximately constant (variation $\lesssim$ 20%) and is about -3 atomic unit for the divalent iron group ions V^{++}, Mn^{++}, Co^{++} and Cu^{++}. Therefore, to the first order approximation, we can regard $\langle r^{-3}\rangle K$ to be roughly constant. Thus,

$$\frac{A(Ni^{61})^{\#}}{A(Co^{59})^{\#}} = \frac{I^{59}}{I^{61}}\frac{\mu_N^{61}}{\mu_N^{59}}\frac{[\langle r^{-3}\rangle K]^{61}}{[\langle r^{-3}\rangle K]^{59}} = \frac{8.3}{54.0}$$

with $I^{59} = \frac{7}{2}$, $I^{61} = \frac{3}{2}$ and $\mu_N^{59} = 4.639$ nm.

$$\mu_N(Ni^{61})^{\#} = 0.31\,\frac{[\langle r^{-3}\rangle K]^{61}}{[\langle r^{-3}\rangle K]^{59}} \simeq 0.31 \text{ nm}.$$

Recently, Heine[47] and Wood and Pratt[48] proposed another mechanism which is equivalent to the above-mentioned Abragam-Horowitz-Pryce configurational mixing mechanism to explain the existence of this anomalous s-electron effect in the observed hyperfine coupling constant. The mechanism is essentially to take into account the exchange interaction of the unpaired 3**d**-electrons with the inner core paired s-electrons. On account of

the difference in the exchange interaction between two electrons with parallel and antiparallel spins the resultant is the net polarization of inner core s-electrons which in turn contribute to the observed hyperfine constant A through the Fermi contact term in the Hamiltonian. In this way, the first principle calculation of $\langle r^{-3} \rangle_K$ is possible; the result for Ni^{++} in a cubic crystalline field is given by Watson and Freeman[49]. The quantity calculated is χ which is related to $\langle r^{-3} \rangle_K$ by

$$\langle r^{-3} \rangle_K = -\frac{2}{3}\chi$$

with $\chi = -3.27$ atomic unit

$$\langle r^{-3} \rangle_K = \left(\frac{2}{3}\right)3.27 = 2.18 \text{ a.u.} = \frac{2.18}{(5.29\times10^{-9})^3} = 1.146\times10^{25} \text{ cm}^{-3}$$

$$A^{61} = 8.3\times10^{-4} \text{ cm}^{-1} = 1.65\times10^{-19} \text{ ergs}$$

since

$$A = -\frac{2\beta\beta_N\mu_N}{I}\langle r^{-3} \rangle_K$$

$$|\mu_N^{61}| = \frac{IA^{61}}{2\beta\beta_N\langle r^{-3} \rangle_K} = \frac{3/2 \times 1.65\times10^{-19}}{2\times0.927\times10^{-20}\times5.05\times10^{-24}\times1.146\times10^{25}} = 0.18 \text{ nm.}$$

This compares reasonably with spectroscopic measurement $|\mu_N| \sim 0.25$ nm. by Kessler[50].

As mentioned earlier, some of these uncertainties can be avoided by means of the double resonance technique, which was used to measure the nuclear parameters of Fe^{57} in silicon.

The resolved ESR hyperfine spectrum for Fe^{57} was obtained

first by Ludwig, Woodbury and Carlson[31]. These investigators diffused several milligrams of iron, enriched in Fe^{57} to 84.1%, into a silicon crystal of dimensions 3 x 3 x 10mm^3. The sample was held at 1200°C for about twenty-four hours. At 10°K, s spectrum of two lines with

$$g = 2.0699$$
$$|A| = 6.984 \times 10^{-4} \text{ cm}^{-1}$$

was observed. To make a precision determination of the magnetic moment, Ludwig and Woodbury[32] carried out an ENDOR experiment. At these low temperatures, earlier investigations had indicated that the ion is in the form Fe°, so that S = 1. Since I = 1/2, the energy level diagram is as shown in Figure 15.

Because silicon has cubic structure, the three electron Zeeman levels are equally spaced. The splitting of each electron level into two levels is due to the nuclear hyperfine interaction. The separations of these levels according to perturbation calculation is given by

$$h\nu = \left| AM - g'_N \beta_N H - \frac{M(2M-1)+S(S+1)-M^2}{2} A^2 \right|$$

For ν = 14,115.4 Mc/sec at H = 4868.6 gauss, resonances were observed at f = 20.943 ± 0.6925 Mc/sec for M = ±1 levels and at 0.7096 Mc/sec for the level M = 0, ±1, it is possible to determine from above expression both the sign and magnitude of g'_N. From these frequencies, after making certain corrections, Ludwig and Woodbury[32] obtained the value

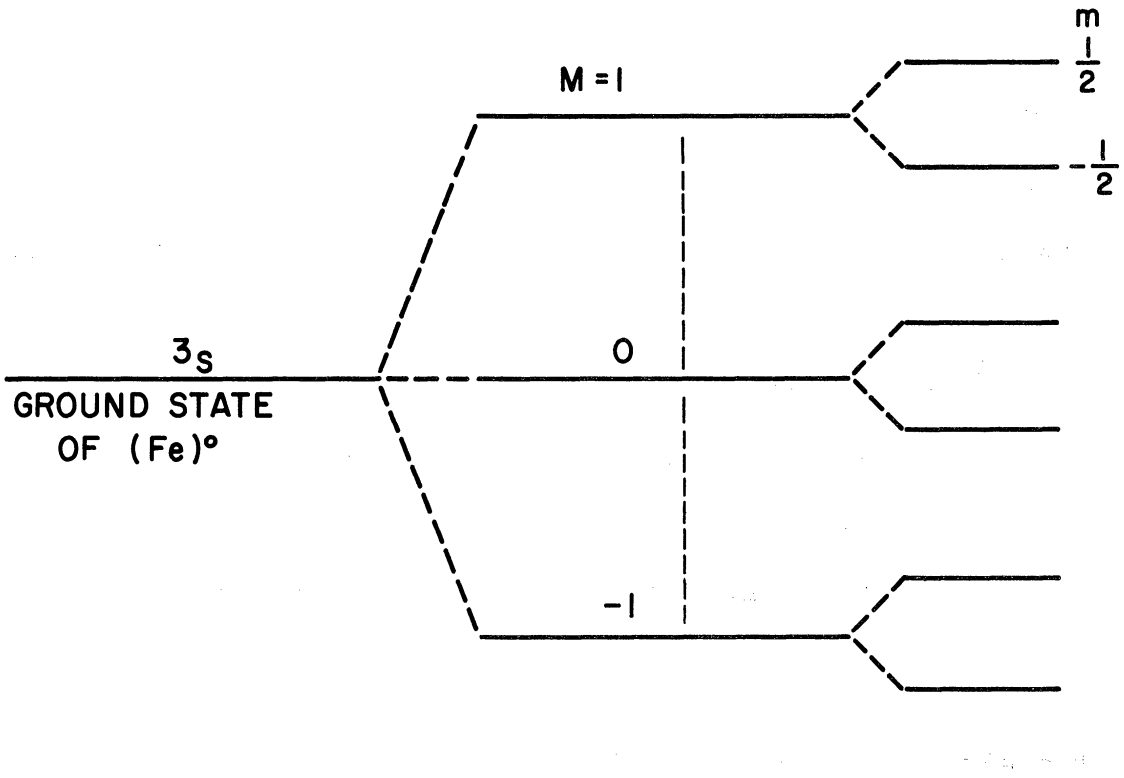

FIG 15

$g_N = +0.1806 \pm 0.0013$ (g_N is the corrected value of g_N')

so that

$$\mu_N(Fe^{57}) = 0.0903 \pm 0.0007 \text{ nm.}$$

B. Electric Quadrupole Moment

Experimental work on the nuclear quadrupole measurements by the ESR method is somewhat scanty at the moment. An example is the work by Terhune, Lambe, Kikuchi and Baker[33], on the quadrupole moment of Cr^{53}. More recently, Eisinger, Blumberg, and Geschwind[34] have attempted to use similar techniques for the measurement of the Cu^{63} and Cu^{65} quadrupole moments. At present, very little definitive information is known about the quadrupole moments of iron group nuclei, so that the double resonance technique to be described here may be a potentially important tool.

The electron nuclear double resonance (ENDOR) technique developed by Feher[14, 15] permits direct measurement of transitions between hfs. levels in the ESR spectra. One can measure values of the interaction parameters with a much greater degree of precision than through observation of hfs. in ESR spectra.

The theory underlying this technique can, perhaps, be understood by reference to the following energy level diagram of Cr^{+++} in ruby (see Figure 16). When the magnetic field is along the

crystal C-axis, the magnetic field dependence of the 4 Zeeman levels for S = 3/2 is given by the two pairs of diverging straight lines. These lines, however, give the energy level of the even-even isotopes of Cr. Only chromium contains about 9.55% Cr^{53}, for which the nuclear I is 3/2, so that for electrons associated with such nuclei, each of the electron spin levels consists of a group of four levels spaced closely together, as indicated by the curly brackets (in Figure 16). The spacings of the hfs. levels depend upon the electron nuclear spin-spin interaction, upon the second order effects arising from the proximity of the electron levels, and also upon the electron-nuclear quadrupole moment interaction.

The spacings of these hfs. levels are measured directly by first applying a saturating microwave as indicated by the double arrow in the diagram. Then, holding the microwave frequency and the magnetic field constant, a second frequency in the r.f. range is applied. Figure 17 gives the schematic of the cavity used for the experiments. The horizontal rectangular piece represents the cavity in which the ruby crystal is placed. The crystal is oriented so that it is accurately parallel to the magnetic field. The saturating microwave power is introduced into the cavity by means of a stainless guide, which is an extension of a conventional ESR spectrometer. The auxiliary r.f. power is applied by means of a loop of wire wound around the crystal. The next figure gives the experimental results that were

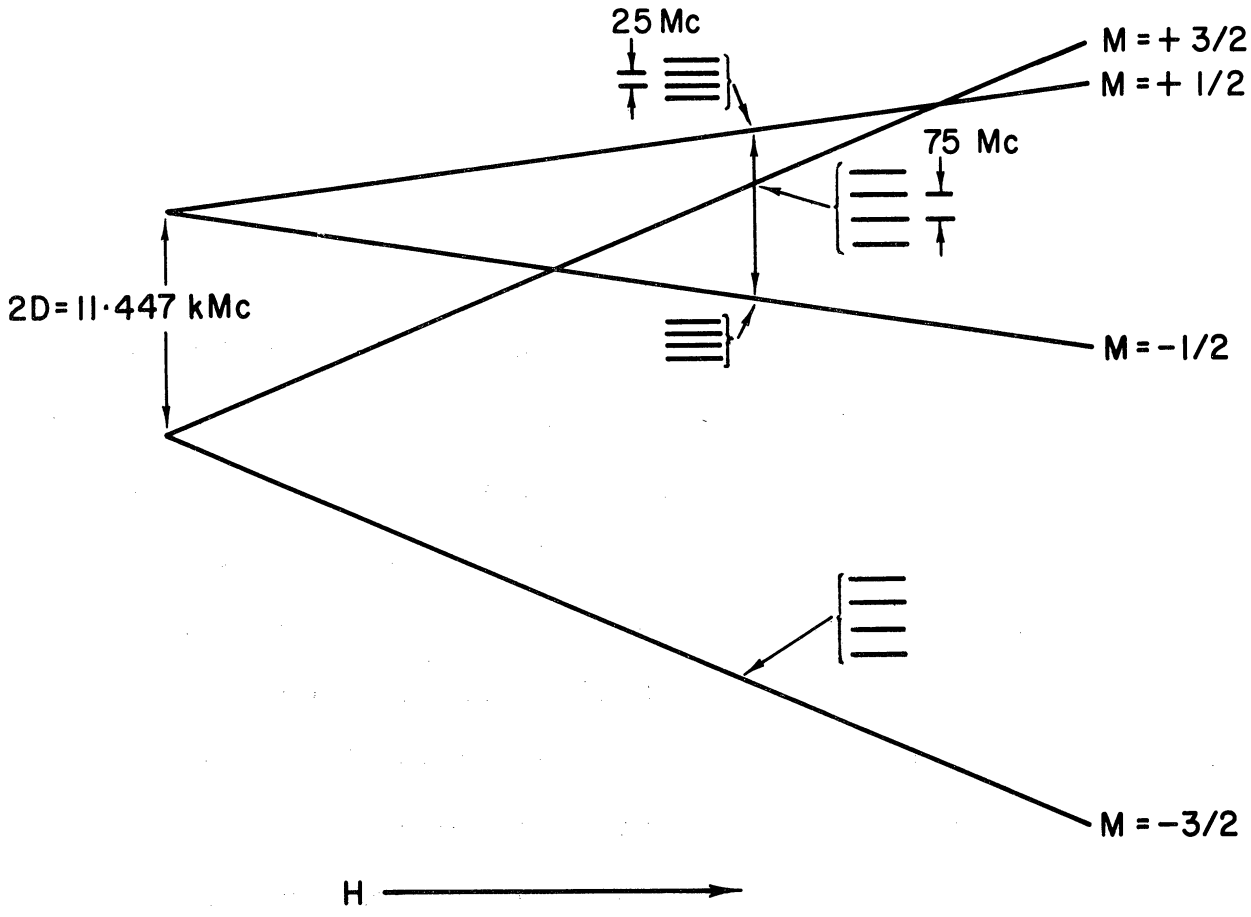

FIG 16

ENERGY LEVELS FOR Cr^{3+} IN Al_2O_3 AT $\theta = 0°$

obtained. We note that the resonance absorption frequencies for the hyperfine transitions of the M = ± 1/2 groups are near 25 Mc/sec, and those for ± 3/2 are approximately three times or near 75 Mc/sec. There is, however, marked variations in the structure of the triplets. These differences stem from second order effects, and nuclear quadrupole interaction.

The quadrupole coupling constant Q , which is evaluated from the experimental spectrum, is related to the quadrupole moment by

$$Q' = \frac{3eQ}{4I(2I-1)}\left(\frac{\partial^2 V}{\partial z^2}\right)_0$$

By means of nuclear quadrupole resonance experiments or by the double resonance experiment described here, it is possible to obtain the corresponding quantity for Al^{27} in the sapphire lattice. In addition, the absolute value of the Al^{27} quadrupole moment is known from atomic beam measurements. If these results are collected together,

$$Q(Cr^{53}) = -0.05 \frac{\left(\frac{\partial^2 V}{\partial z^2}\right) \text{at the } Al^{27} \text{ site}}{\left(\frac{\partial^2 V}{\partial z^2}\right) \text{at the } Cr^{53} \text{ site}} .$$

For paramagnetic ions in solids, the gradient of the electric field at the nuclei contains a contribution from the dis-

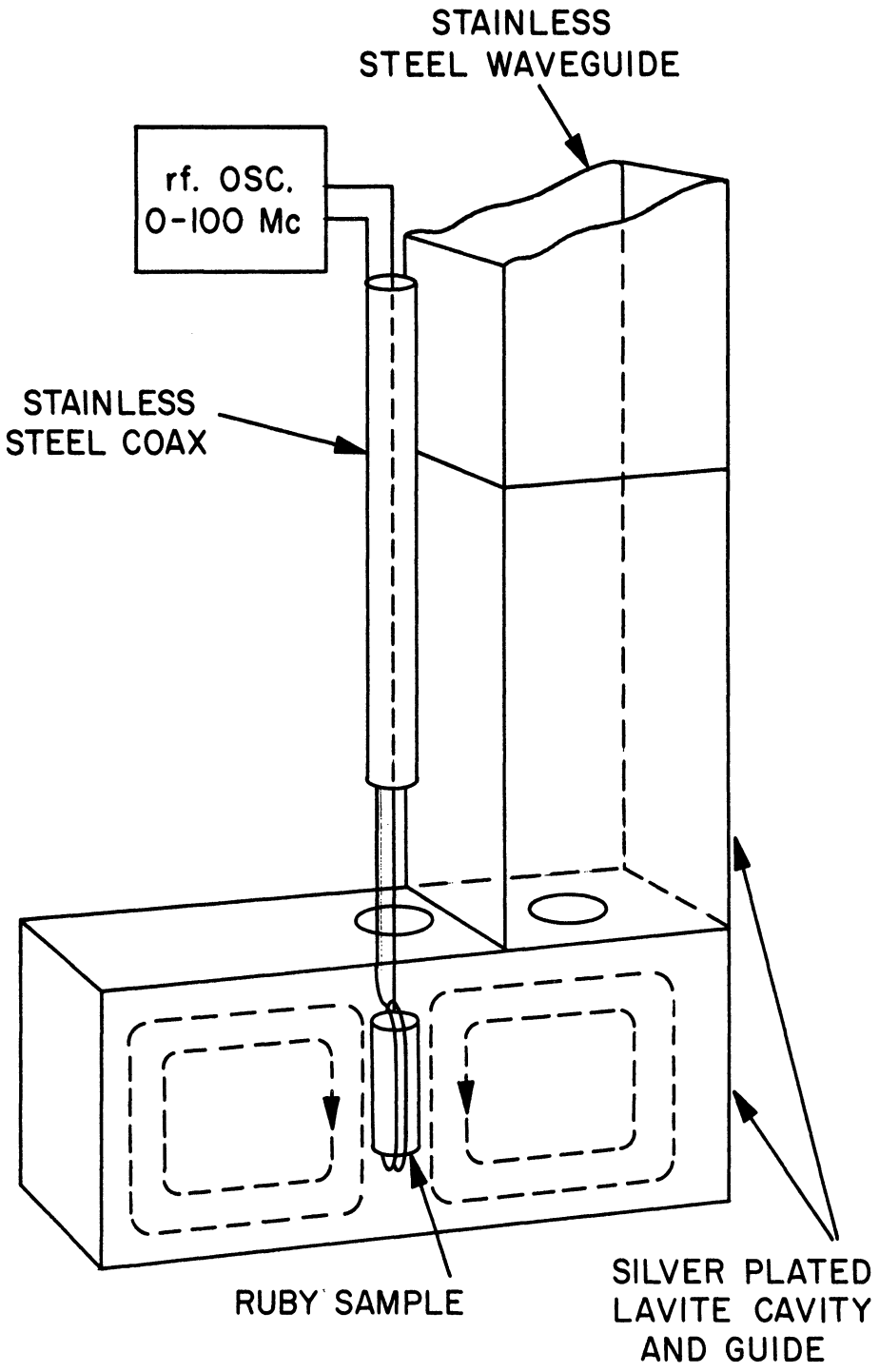

FIG 17

APPARATUS USED IN MAKING
ELECTRON NUCLEAR DOUBLE RESONANCE MEASUREMENTS

torted electron cloud and from the crystalline electric field. However, in the case of the Cr^{+++} ion, the electronic g value is almost isotropic and, according to Abragam and Pryce[6], the electronic contribution to the electric field gradient is negligible. Thus, as a first approximation, the electric field gradients at both the Al^{27} and Cr^{53} nuclei are associated with the same crystalline electric field. The ratio of the field gradients at the two nuclear sites would then be equal to the ratio of antishielding factor $(1 - \gamma_\infty)$ for the two ions. For Al this factor is about 3.59, and for Cr^{+++} it is estimated to be about 6. These results then give

$$Q(Cr^{53}) = -0.03 \text{ barn}$$

for the electric quadrupole moment.

While the accuracy of this determination of Q for Cr^{53} is quite limited, this method appears promising for obtaining quadrupole moments of the ion group elements, many of which have not yet been measured. Studies of systems, such as vanadium in which ions of several different valence states can be observed, would be of particular importance in reducing many of the uncertainties.

V. Applications to Solid-State Chemistry

In the magnetic moment measurement of Ni^{61}, it was pointed out that the unusual valence state Co^{+} was produced in MgO by means of x-irradiation. A variety of investigations of this type

have been carried out in different laboratories. For example, Wertz and Auzins[11] noted that the Cr^{3+} signal in MgO is reduced upon x-irradiation, while that of Fe^{3+} increases. These changes in the ESR spectrum intensities are not due to atomic displacements, because the original intensity can be restored readily by heat treatment. These changes are due to transfer of electrons from one center to another.

These observations then, suggest that it might be possible to develop ESR as an analytical tool to determine changes in oxidation states brought about by x-rays and other high energy radiations. As these ionizing radiations proceed through the crystalline lattice, a cloud of electron dust is set up, and the electrons can become trapped at metastable centers. As a result, rather unusual valence states can be produced.

A good example for discussion is vanadium sapphire, investigated by Lambe and Kikuchi[35]. The vanadium in this material is identified by means of the characteristic 8 hfs. (V^{51}, 99.75%, I = 7/2) lines. The specific valence state is then determined from the angular dependence, and the temperature dependence of the vanadium spectrum. The vanadium in sapphire occurs as a chemical impurity occupying the Al substitutional sites. Since aluminum is Al^{3+} we can expect the normal valence state of vanadium to be V^{+3}. That this is the case can be readily verified by experiment.

The electron spin of V^{+3} is 1 so that in an axial crystalline electric field splits the ground state into a singlet (M = 0) and a doublet (M = ±1), separated by about 10 cm^{-1}. Because the separation is large, at microwave frequencies, only transitions between the M = ±1 levels are observed. By making measurements at liquid HeI and liquid HeII temperatures, it can be readily verified that the states M = ±1 lie above the level M = 0. The spectrum is strongly angle dependent, and the hfs. components are about 110 gauss apart.

In addition to the V^{+3} spectrum that can be seen only at low temperatures, it is possible to observe, under high gain, a set of 8 isotropic lines having component separations of about 140 gauss. This spectrum has been assigned to V^{4+} (S' = 1/2).

If the vanadium sapphire crystal is subjected to ionizing radiation, a spectrum is developed that can be readily ascribed to V^{2+}. This assignment follows from the fact that there are three groups of eight lines, with hfs. separation of about 88 gauss. The V^{2+} centers can be destroyed upon heating at temperatures of about 700°C. The electrons responsible for the changes in the vanadium oxidation state is still a puzzle. Apparently the electrons do not come from the other vanadiums, because the intensity of the V^{4+} lines does not increase with x-irradiation.

This investigation suggested the study of vanadium in several crystalline materials. The properties of the VO^{2+} radicals ori-

ented in a Tutton salt are being investigated* and these results are being used to obtain information about VO^{2+} on organic resins and in glasses.

In passing, we should like to point out that vanadium sapphire is an excellent material to show students certain basic ideas about quantum mechanics. As has been pointed out, the hfs. can be studied and the effects produced by ionizing radiation can be investigated. The Spin Hamiltonian is simple enough so that a student can learn how to make calculations in a very short length of time.

Also, vanadium sapphire can be used to demonstrate vividly the effects of perturbing energy levels crossing over. For example, Figure 18 shows the spectrum obtained at high magnetic field when the magnetic field is along the crystal c-axis. There are eight lines, characteristic of V^{51}. This set of lines is due to the transitions $M = 1/2 \rightarrow 3/2$. The two electron levels are sufficiently removed from other electron levels so that the effects of perturbation are small, and the hfs. lines therefore are of almost equal intensities and equal spacings.

If we go to a slightly lower magnetic field, we should expect to see the lines due to the transitions $M = -1/2 \rightarrow 1/2$. Normally, we would have expected this set to consist of eight

---

*R. Borcherts, G. Wepfer, and C. Kikuchi, to be published.

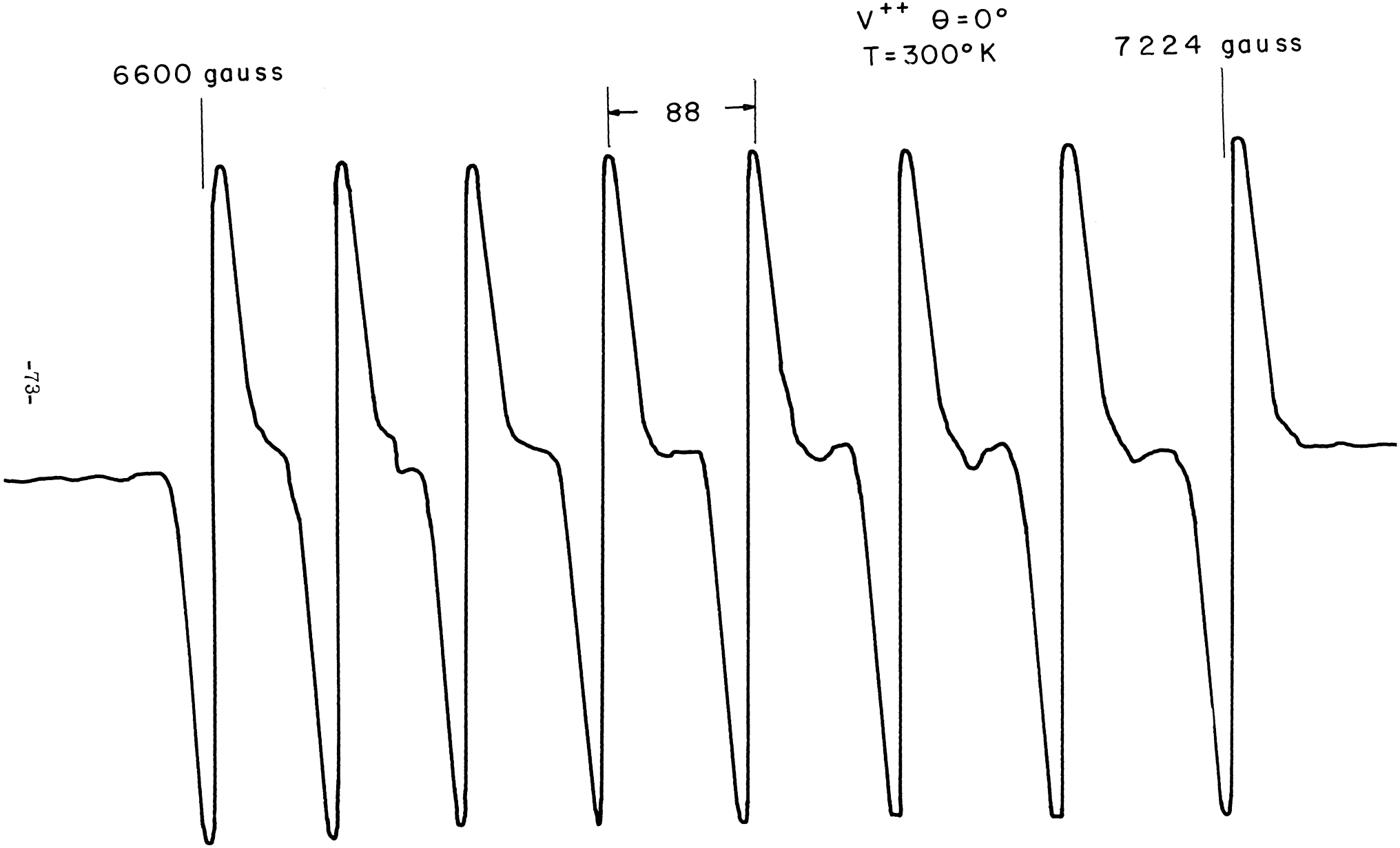

FIG 18

lines. The experimentally observed spectrum near 9, 400 Mc/sec is shown in Figure 19. The spectrum is very complex. The reason for the complex spectrum is easy to see upon inspection of the energy level diagram (see Figure 20). We note that here we are making observations on transitions where the electron levels M = 1/2 and 3/2 would cross over for I = 0. The manner in which the energy levels interact in this vicinity is shown in Figure 21. The reality of the effects of cross-over can be made clearer by taking the spectrum at K-band frequencies. At this frequency $h\nu \gg 2D$ so that the spectrum consists of three groups of eight lines, as shown in Figure 22.

The effects of ionizing radiation on vanadium can be shown also by the following method. If powders of oxides of cubic crystals, such as MgO and CaO are melted with $VOCl_2$, dried, and fired, at first no evidence of vanadium is obtained. However, if the powder sample is subjected to x-irradiation, the eight lines characteristic of vanadium are obtained.

It should be noted that these electron transfer processes can be brought about by optical radiation. The first observation of this was made by Lambe and Kikuchi[36]. In this experiment, a single crystal of CdS containing a small concentration of Fe was placed in the cavity at 4.2°K, and the crystal was illuminated through a hole on the side of the cavity. When the crystal is illuminated with green light, a spectrum which can be identified as due to Fe^{3+} is obtained. If the crystal is then

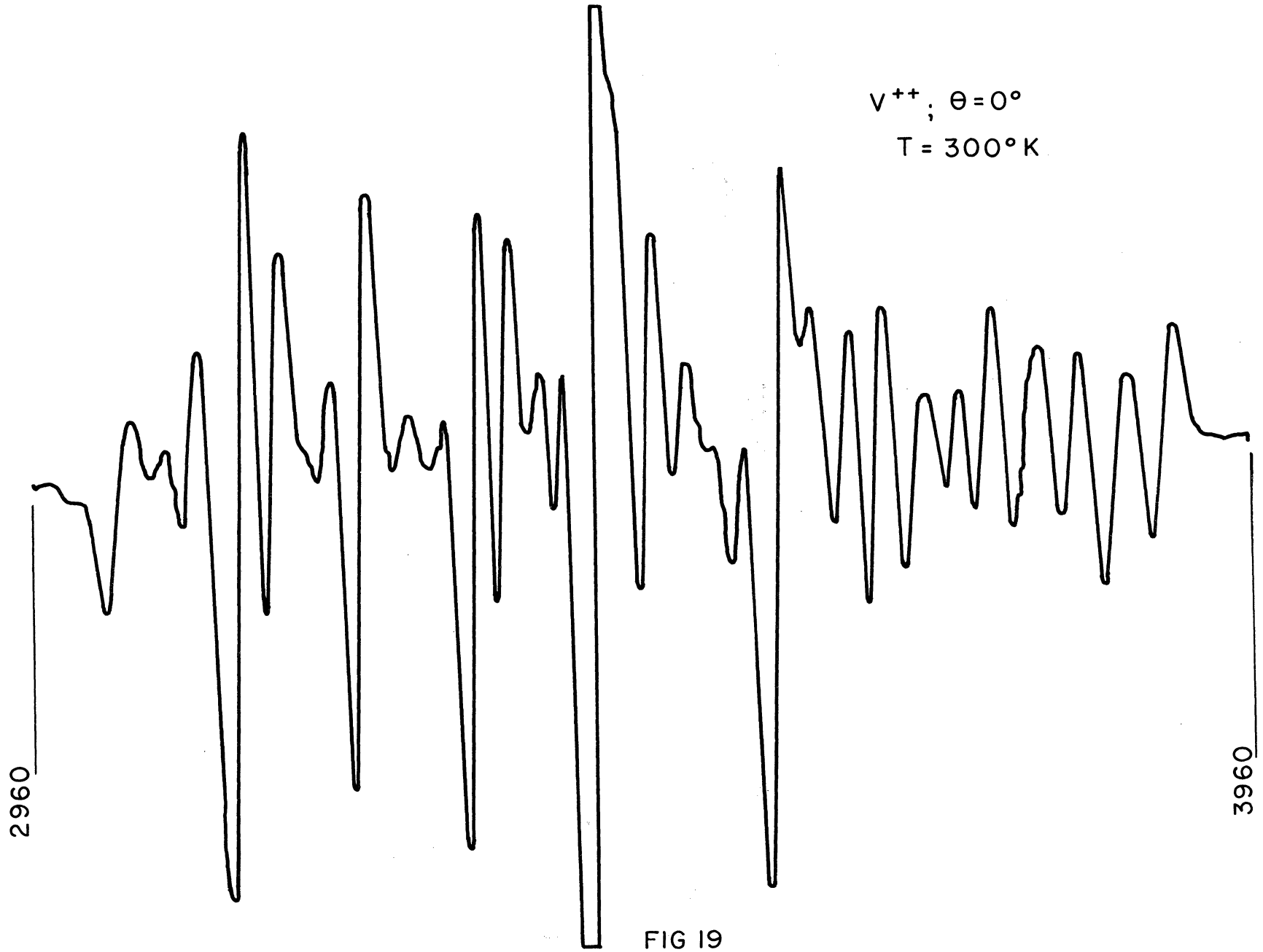

FIG 19

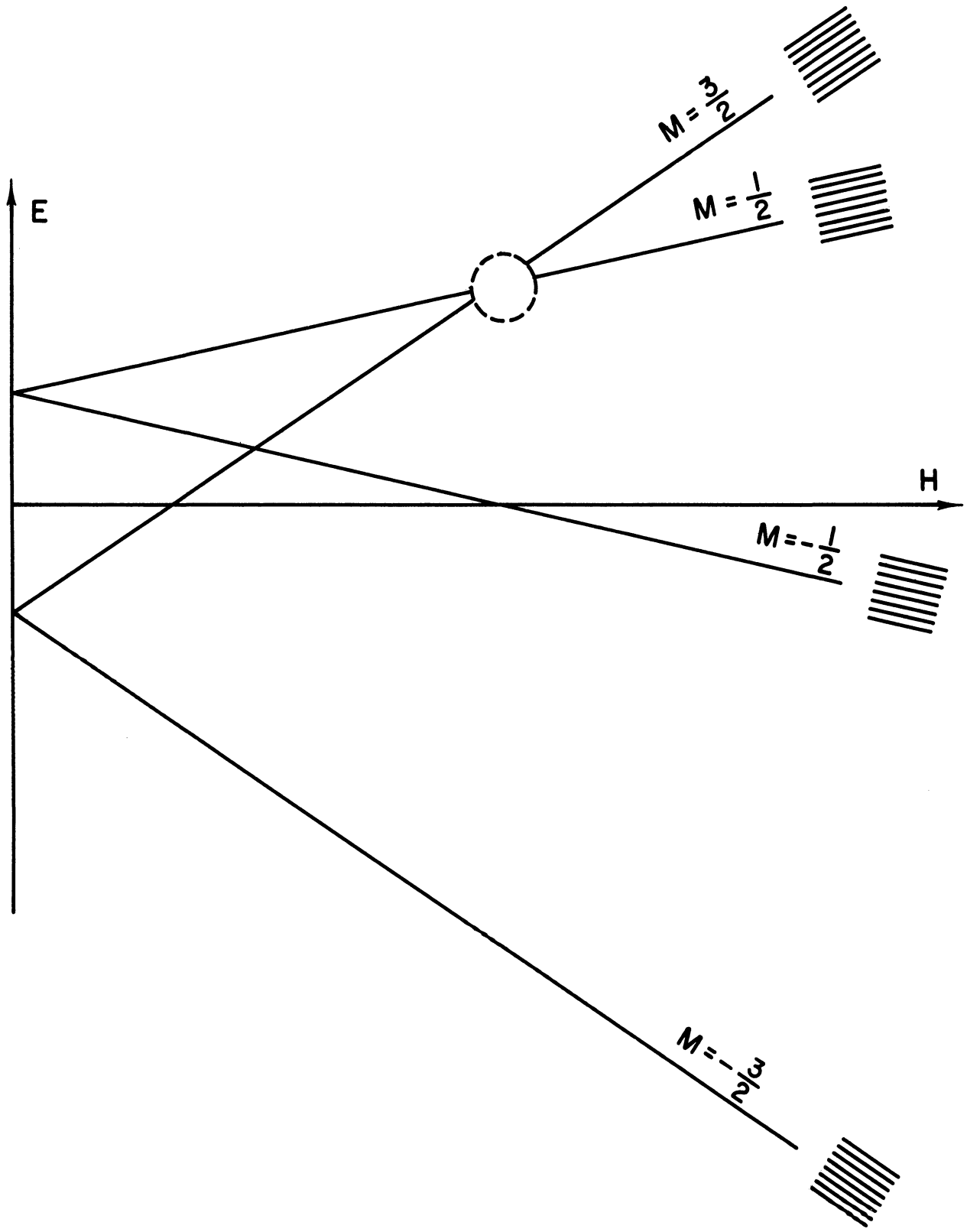

FIG 20

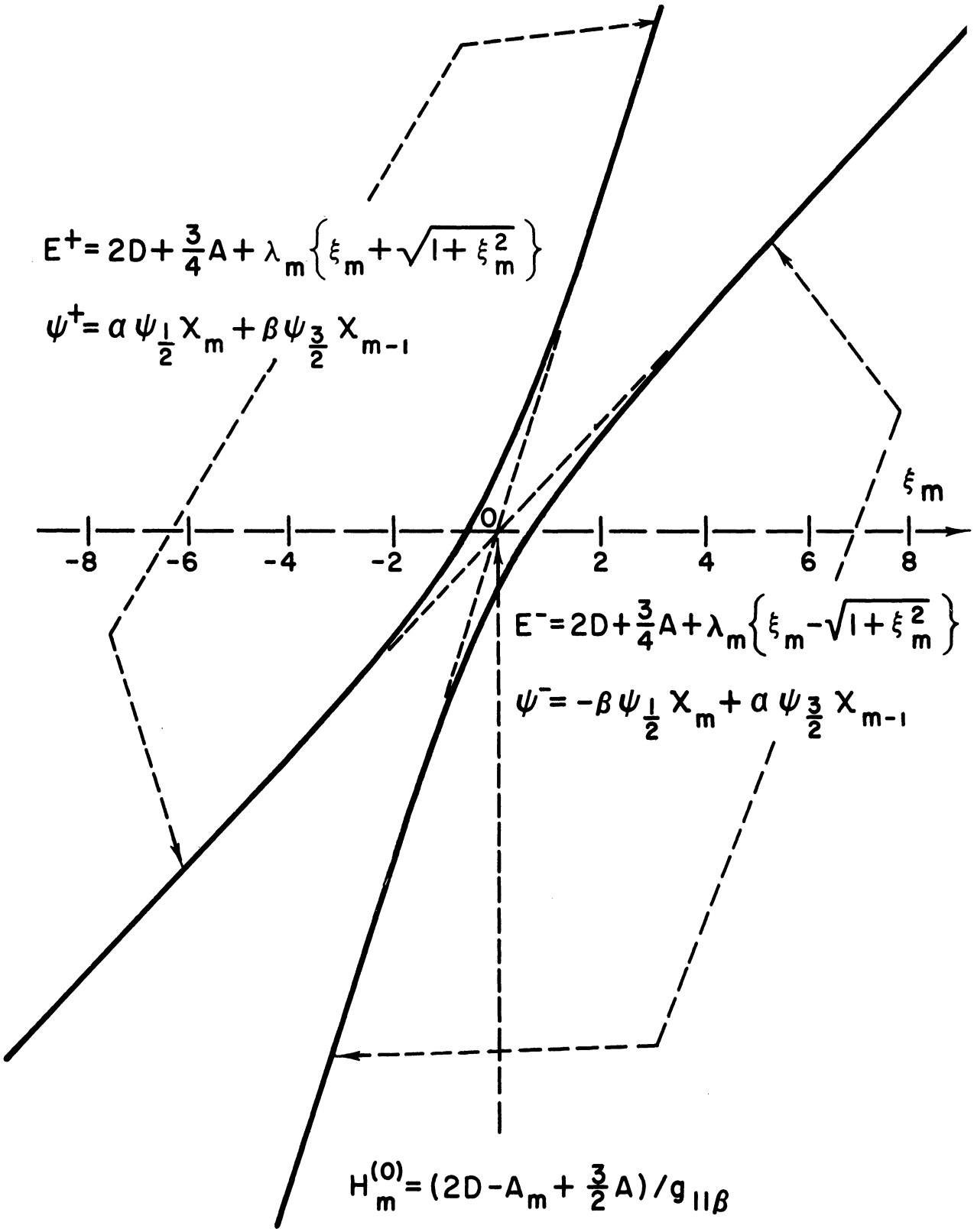
$E^{+}=2D+\frac{3}{4}A+\lambda_m\left\{\xi_m+\sqrt{1+\xi_m^2}\right\}$
$\psi^{+}=\alpha\psi_{\frac{1}{2}}X_m+\beta\psi_{\frac{3}{2}}X_{m-1}$
ξ_m
0
-8
-6
-4
-2
2
4
6
8
$E^{-}=2D+\frac{3}{4}A+\lambda_m\left\{\xi_m-\sqrt{1+\xi_m^2}\right\}$
$\psi^{-}=-\beta\psi_{\frac{1}{2}}X_m+\alpha\psi_{\frac{3}{2}}X_{m-1}$
$H_m^{(0)}=(2D-A_m+\frac{3}{2}A)/g_{11\beta}$

FIG 21

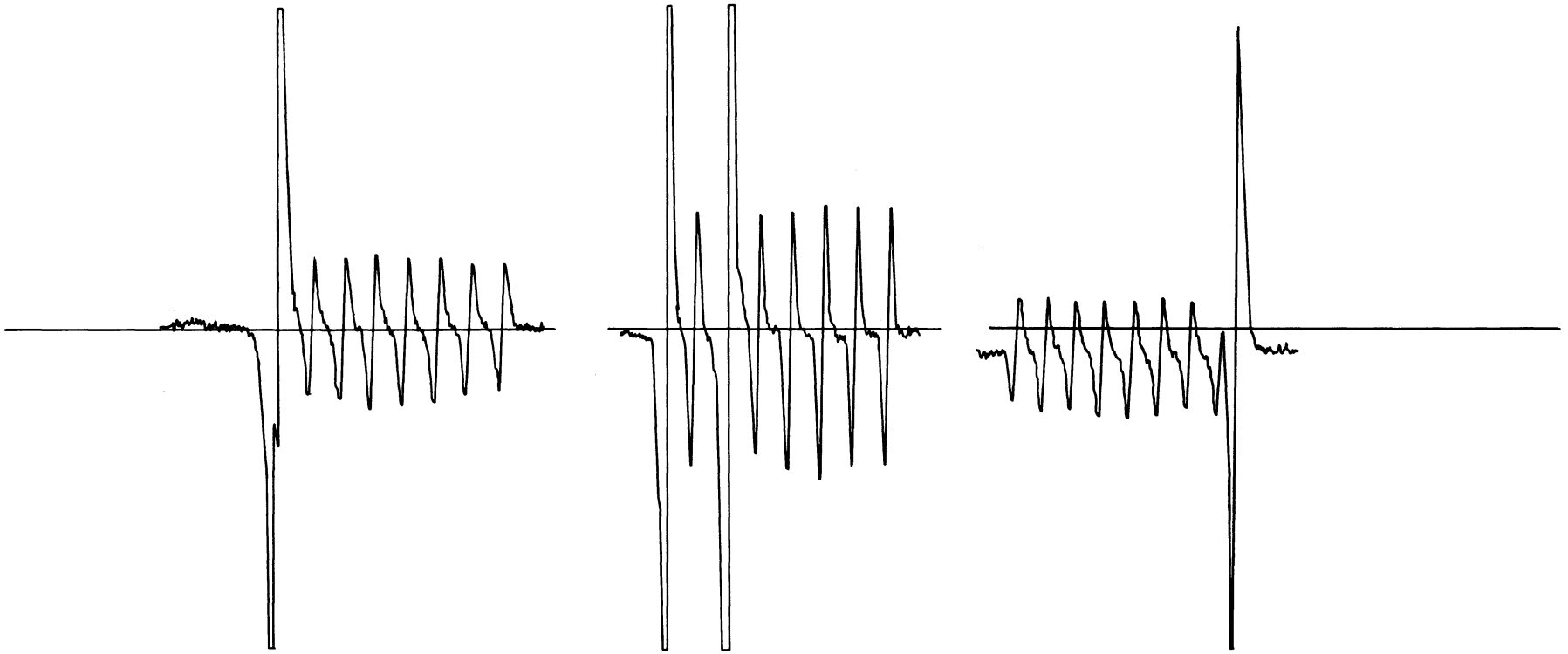

FIG 22

GREEN SAPPHIRE IRRADIATED BY Co-60 GAMMA RAYS

illuminated with red light, the signal disappears.

The interpretation that has been given is as follows: Fe^{2+} is present in CdS as an impurity. Its spin resonance is not observed, possibly being too broad. When free electrons and holes are produced by the green radiation, the Fe^{2+} traps a hole and becomes Fe^{3+}, which is readily observed because it is in the s-state. The electrons must be trapped elsewhere. The action of the two micron infra-red radiation is then to restore the electron back to the Fe^{3+} converting it to Fe^{2+}. The two micron light may release an electron from some other trap or may move it from the valence band into the Fe^{3+}. A similar effect in ZnS:Gd has been observed by R. S. Title[37].

The above examples demonstrate the usefulness of electron spin resonance. No doubt many more applications will be found that will provide us with an insight into the microscopic effects produced by radiations.

APPENDIX A

A HAMILTONIAN FOR ELECTRONS

In this appendix we obtain a Hamiltonian for electrons in an atom. We follow Slater's approach in applying Dirac's theory to a single electron moving in electric and magnetic fields[7]. Generalizations can then be made to take into account the effects due to the nucleus and other electrons, as well as external perturbations. Nuclear motion will be ignored, although, if desired, reduced electronic mass can be used.

It is known that the energy of an electron moving under the influence of external fields is given by the relativistic expression

$$(\mathcal{H} + e\varphi)^2 - m_o^2 c^4 - \left(\underline{p} + \frac{e}{c}\underline{A}\right)^2 = 0, \tag{A-1}$$

where φ , $\underline{A}$ are the scalar and vector potentials, and m_o, $\underline{P}$ are the rest mass and linear momentum of the electron. Here the energy is represented by the Hamiltonian function $\mathcal{H}$. Transition to a quantum mechanical expression is achieved by the usual replacements, $\mathcal{H} \rightarrow i\hbar \frac{\partial}{\partial t}$, $\underline{P} \rightarrow -i\hbar \underline{\nabla}$. However, in order to admit wave solutions having time dependence of the form exp ($-i\varepsilon t/\hbar$) it is necessary that the equation contains only first-order time derivative. For this reason, Dirac chose, instead of the normal Schrodinger equation,

(A-2) $$\left\{ (\mathcal{H}+e\varphi)c^{-1} + \underline{\alpha}\cdot(\underline{P}+\frac{e}{c}\underline{A}) + \beta m_0 c \right\}\psi = 0 ,$$

which also exhibits the space-time symmetry familiar in relativity. The dimensionless quantities $\underline{\alpha}$, β are independent of time and coordinates because in the absence of fields the Hamiltonian must describe a free particle. Therefore, they commute with $\mathcal{H}$, φ, $\underline{P}$, $\underline{A}$.

It is clear that we can also derive a relativistic Schrodinger equation from (1),

(A-3) $$\begin{aligned} i\hbar\frac{\partial\psi}{\partial t} &= \left\{ \left[m_0^2c^4 + (\underline{P}+\frac{e}{c}\underline{A})^2c^2 \right]^{1/2} - e\varphi \right\}\psi \\ &= \left\{ m_0c^2 + \frac{1}{2m_0}\underline{\pi}^2 - \frac{1}{8m_0^3c^2}\pi^4 + \cdots - e\varphi \right\}\psi , \end{aligned}$$

where $\underline{\pi} = (-i\hbar\underline{\nabla} + \frac{e}{c}\underline{A})$, and as in (1), e represents the magnitude of the electronic charge. If (2) is a correct description of the electron then it is reasonable to expect its solution to satisfy (3). In this manner $\underline{\alpha}$ and β can be determined through the requirements

(A-4) $$\begin{aligned} \alpha_i^2 = \beta^2 = 1 , \quad i = 1,2,3 \\ [\alpha_i, \alpha_j]_+ = [\alpha_i, \beta] = 0 , \quad i \neq j \end{aligned}$$

where $[\,]_+$ denotes anticommutator. These conditions cannot be satisfied by ordinary numbers, but if the quantities are treated as matrices then it can be shown that[41]

(A-5) $$\underline{\alpha} = \begin{pmatrix} 0 & \underline{\sigma} \\ \underline{\sigma} & 0 \end{pmatrix}, \quad \beta = \begin{pmatrix} \mathbb{1} & 0 \\ 0 & -\mathbb{1} \end{pmatrix},$$

where σ_i are the well-known Pauli matrices and $\mathbb{1}$ is a unit matrix of rank 1. This result means that (2) becomes a matrix equation and that ψ is now a four component column vector,

(A-6) $$\begin{pmatrix} \epsilon_+ & 0 & \pi_3 & \pi_1 - i\pi_2 \\ 0 & \epsilon_+ & \pi_1 + i\pi_2 & -\pi_3 \\ \pi_3 & \pi_1 - i\pi_2 & \epsilon_- & 0 \\ \pi_1 + i\pi_2 & -\pi_3 & 0 & \epsilon_- \end{pmatrix} \begin{pmatrix} \psi_1 \\ \psi_2 \\ \psi_3 \\ \psi_4 \end{pmatrix} = 0,$$

where $\epsilon_\pm = (\mathcal{E} + e\varphi)c^{-1} \pm m_0 c$. Since the determinant formed by coefficients of ψ_i must vanish we obtain equation (1) with $\mathcal{H} = \mathcal{E}$. $\mathcal{E}$ appears quadratically so there are two energy eigenvalues, one positive and the other negative; it can be shown that there are two linearly independent solutions (2 sets of ψ_i) corresponding to each choice of the energy.*

For electrons we choose the positive energy and eliminate ψ_1 and ψ_2 after rewriting (6) as four equations. The two remaining equations containing ψ_3 and ψ_4 can be reduced by operating π_i on all functions depending upon positions. After some manipulation, each of the two equations is found to be a com-

---

* Negative energy corresponds to positions.

ponent of the equation[7].

$$\left\{ \frac{\left(\underline{P}+\frac{e}{c}\underline{A}\right)^2}{2m_0+(E'+eQ)c^{-2}} + \frac{e\hbar c^{-1}(\underline{H}\cdot\underline{\sigma})}{2m_0+(E'+eQ)c^{-2}} - eQ \right.$$

$$\left. - \frac{ie\hbar c^{-2}}{\left[2m_0+(E'+eQ)c^{-2}\right]^2}\underline{E}\cdot\left[\left(\underline{P}+\frac{e}{c}\underline{A}\right)+i\left(\underline{P}+\frac{e}{c}\underline{A}\right)\times\underline{\sigma}\right]\right\}\psi = 0 \,, \tag{A-7}$$

where $E' = \mathcal{E} - m_0c^2$, the potentials are assumed to be time-independent, and ψ is a two-component column vector. The Hamiltonian given by equation (7) represents the energies of a single electron moving in electric and magnetic fields. We shall next specify the various fields and potentials, and thus introduce electrostatic and magnetic interactions arising from the presence of other electrons in the atom and the nucleus. At the same time, the Hamiltonian can be generalized to describe an arbitrary number of electrons.

Consider a many-electron ion in which the positions of the nucleus and the jth electron are specified by $\underline{R}$ and $\underline{r}_j$. At any electron the magnetic field is the sum of effects due to the orbital motion of the electron, the magnetic moments of the nucleus and other electrons. For this electron the scalar potential will consist of Coulomb interactions with the nucleus and other electrons. If the ion is placed in a crystalline lattice then the neighboring oppositely-charged ions produce an external field which must be included. Consequently, the interaction

energies of the jth electron becomes

$$
\begin{aligned}
(A\text{-}8)\qquad \mathcal{H}_j = &\left[2m_0+(E'+e\phi_j)c^{-2}\right]^{-1}\left\{ P_j^2 + \frac{2e}{c}\underline{P}_j\cdot\left(\underline{A}_{ext.}+\underline{A}_{Nj}+\sum_k{}' \underline{A}_{jk}\right)\right. \\
&\left. +\left(\frac{e}{c}\underline{A}_j\right)^2 + e\hbar c^{-1}\underline{\sigma}_j\cdot\left(\underline{H}_{ext}+\underline{H}_{Nj}+\sum_k{}'\underline{H}_{jk}\right)\right\} \\
&-\left\{e\phi_{ext}+\frac{Ze^2}{|\underline{R}-\underline{r}_j|}-\sum_k{}' e^2 r_{jk}^{-2}\right\} - ie\hbar\left[2m_0c+(E_j'+e\phi_j)c^{-2}\right]^{-2} \\
&(x)\left\{\left[\underline{E}_{ext}+\frac{Ze(\underline{R}-\underline{r}_j)}{|\underline{R}-\underline{r}_j|^2}-e\sum_k{}'\underline{r}_{jk}r_{jk}^{-3}\right]\right. \\
&\left.\cdot\left[(\underline{P}_j+\frac{e}{c}\underline{A}_j)+i(\underline{P}_j+\frac{e}{c}\underline{A}_j)\times\underline{\sigma}_j\right]\right\},
\end{aligned}
$$

where $\underline{r}_{jk}=\underline{r}_j-\underline{r}_k$ and $\underline{H}_{ext}$ represents the external magnetic field. In this expression nuclear-electron and electron-electron terms are denoted by subscripts N and jk respectively, the primed summation symbol implies that terms with k = j are to be omitted. The scalar potential, as we have written, is not quite correct because of retardation effects and the fact that electrons are in motion. However, the necessary modification does not effectively alter the Hamiltonian for our purposes so we shall neglect the corrections. The total Hamiltonian can therefore be written as a sum of $\mathcal{H}_j$ if one is careful not to double count the terms involving electron-electron interactions. This remark will be made

explicit in the following.

From classical electromagnetic theory it is known that the vector potential and magnetic field at the jth electron due to the presence of the kth electron are given by

$$\underline{A}_{jk} = \underline{J}_k r_{jk}^{-1} + (\underline{\mu}_k \times \underline{r}_{jk}) r_{jk}^{-3}, \tag{A-9}$$

$$\underline{H}_{jk} = (\underline{J}_k \times \underline{r}_{jk}) r_{jk}^{-3} - \underline{\mu}_k r_{jk}^{-3} + 3\underline{r}_{jk}(\underline{\mu} \cdot \underline{r}_{jk}) r_{jk}^{-5}, \tag{A-10}$$

d

where $\underline{J}_k$ and $\underline{\mu}_k$ are the current density and magnetic moment of the kth electron. In the quantum description, $\underline{J} = -\frac{e}{m_o c}\underline{P}$ and $\underline{\mu} = -\beta\underline{\sigma}$, where $\beta = \frac{e\hbar}{2m_o c}$ is the Bohr magneton. For the nucleus with angular momentum $\underline{I}$ the associated magnetic moment $\underline{\mu}_N$ is $g_N\beta_N\underline{I}$, where g_N and β_N are nuclear gyromagnetic ratio and nuclear magneton respectively. Equations (9) and (10) can then be used to give $\underline{A}_{Nj}$ and $\underline{H}_{Nj}$.

For convenience, we shall represent the terms in each curly bracket in (8) by $(\mathcal{H}_j)_i$, i = 1,2,3. To a good approximation the denominator in $(\mathcal{H}_j)_1$ can be replaced by $2m_o$. Since the leading term, the kinetic energy, is the largest term in the Hamiltonian we can obtain a better approximation by expanding its denominator in powers of c^2,

$$P_j^2\left[2m_o + (E_j' + eq_j)c^{-2}\right]^{-1} \simeq P_j^2\left[2m_o + \frac{P_j^2}{2m_o c^2}\right]^{-1} \tag{A-11}$$

$$\underline{\sim} \frac{P_i^2}{2m_0} - \frac{P_i^4}{8m_0^3c^2},$$

where the second term clearly represents the relativistic correction to the kinetic energy. Hence

$$(\mathcal{H}_i)_1 = \frac{P_i^2}{2m_0} - \frac{P_i^4}{8m_0^3c^2} + eg_N\beta_N(\underline{I}\times\underline{r}_i)\cdot\underline{P}_i(m_0cr_i^3)^{-1}$$

(A-12)
$$+ g_N\beta_N\beta\left[3(\underline{I}\cdot\underline{r}_i)(\underline{\sigma}_i\cdot\underline{r}_i)r_i^{-5} - (\underline{I}\cdot\underline{\sigma}_i)r_i^{-3}\right] + \beta\underline{\sigma}_i\cdot\underline{H}_{ext}$$

$$- \frac{e\beta}{m_0c}\sum_k{}' \left[2(\underline{P}_i\cdot\underline{P}_k)(\hbar r_{ik})^{-1} + \left\{(\underline{\sigma}_k\times\underline{r}_{ik})\cdot\underline{P}_i + (\underline{\sigma}_i\times\underline{r}_{ik})\cdot\underline{P}_k\right\}r_{ik}^{-3}\right.$$

$$\left. -\hbar(\underline{\sigma}_i\cdot\underline{\sigma}_k)(2r_{ik}^3)^{-1} + 3\hbar(\underline{\sigma}_i\cdot\underline{r}_{ik})(\underline{\sigma}_k\cdot\underline{r}_{ik})(2r_{ik}^5)^{-1}\right]$$

$$+ \frac{e}{m_0c^2}(\underline{P}_i\cdot\underline{A}_{ext}),$$

where we have assumed that the nucleus is sufficiently close to the origin as compared to the electrons so that $|\underline{R}-\underline{r}_i| \sim r_i$, and terms of order A_i^2 have been neglected. It is seen that terms contained in the k-summation represent electron-electron magnetic interactions; they are symmetric in the indices and therefore constitute the total contribution to the Hamiltonian from the jkth pair. When summing over all electrons to obtain the total Hamiltonian we must multiply these terms by a factor

of 1/2 to avoid double counting. The nuclear-electron interactions in (12) can be rearranged as:

$$2g_N\beta_N\beta\,\underline{I}\cdot\left[(\underline{l}_j-\underline{s}_j)r_j^{-3}+3\underline{r}_j(\underline{s}_j\cdot\underline{r}_j)r_j^{-5}\right], \tag{A-13}$$

with $\underline{\sigma}_j=2\underline{s}_j$, $\hbar\underline{l}_j=\underline{r}_j\times\underline{p}_j$. Terms in the bracket may be regarded as the effective magnetic field at the nucleus produced by the jth electron.

Electrostatic energies are given $(\mathcal{H}_j)_2$. The various electric-multipole interactions can be displayed by expanding the nuclear electron Coulomb term in inverse powers of r_j. Keeping terms up to r_j^{-5} we obtain

$$(\mathcal{H}_j)_2=-e\ell_j=-e\ell_{ext}+e^2\sum_k{}' r_{jk}^{-1} \tag{A-14}$$
$$-Ze^2\left[r_j^{-1}+(\underline{r}_j\cdot\underline{R})r_j^{-3}+\{3(\underline{r}_j\cdot\underline{R})^2-r_j^2R^2\}(2r_j^3)^{-1}\right].$$

The three terms arising from the expansion correspond to the ordinary Coulomb, dipole, and quadrupole interactions respectively. From parity consideration it is readily seen that the nucleus has no dipole moment and so the second term must vanish.

The terms in $(\mathcal{H}_j)_3$ are effects involving the electric field $\underline{E}_j$. We note that the electron-electron contribution is not symmetric in j and k, thus in the total Hamiltonian we need to add a similar term interchanging j with k. It was seen earlier that $\underline{R}-\underline{r}_j$ may be taken to be $\underline{r}_j$ such that the electric field arising from nuclear-electron interaction can be treated as a

central field. Since we are already dealing with a small contribution to the Hamiltonian we may neglect most terms in $\underline{A}_j$ in comparison with $\underline{P}_j$. The only vector potential we will retain is $\underline{A}_{Nj}$ because the inclusion of this term leads to a nuclear-electron coupling due only to the S-state electrons $(\ell_j = 0)$ for which the nuclear-electron interactions in $(\mathcal{H}_j)_1$ vanish. To illustrate this remark let us write

$$(\mathcal{H}_j)_3 = -\frac{ie\hbar}{4m_0^2c^2}\Big[\underline{E}_{ext}\cdot(\underline{P}_j + i\underline{P}_j\times\underline{\sigma}_j) + Ze\,\underline{r}_j\cdot(\underline{P}_j + i\underline{P}_j\times\underline{\sigma}_j)r_j^{-3}$$

(A-15)

$$- e\sum_k{}' \underline{r}_{jk}\cdot(\underline{P}_j + i\underline{P}_j\times\underline{\sigma}_j)r_{jk}^{-3}\Big]$$

$$+ \frac{e^2\hbar}{c}\left[2m_0c + (E_j' + eq_j)c^{-2}\right]^{-2} E_j\,\hat{\underline{r}}_j\cdot(\underline{A}_{Nj}\times\underline{\sigma}_j),$$

where we have replaced the denominator by $2m_0$ except in the last term for which we assume $\underline{E}_j = E_j\hat{\underline{r}}_j$.* This last approximation is usually valid since nuclear electron effects generally dominate.

The reason for retaining the full denominator in the nuclear term in (15) can be seen when we consider the fact that ultimately the quantity of interest is an averaged Hamiltonian. Using the vector identities the operators become,

---

* The term proportional to $\underline{E}_j \cdot \underline{A}_{N_j}$ therefore vanishes.

$$\underline{r}_j \cdot (\underline{A}_{Nj} \times \underline{\Gamma}_j) = 2g_N \beta_N \underline{s}_j \cdot \underline{r}_j \times (\underline{I} \times \underline{r}_j) r_j^{-3}$$
$$= 2g_N \beta_N \underline{I} \cdot [\underline{s}_j r_j^{-1} - \underline{r}_j (\underline{r}_j \cdot \underline{s}_j) r_j^{-3}] .$$

The small nuclear magnetic moment enables us to apply perturbation theory. Therefore, to first order we will be interested in the diagonal matrix elements of $(\mathcal{H}_j)_1$ in the representation which diagonalizes $\underline{j}_j^2 = (\underline{l}_j + \underline{s}_j)^2$, the square of jth electronic angular momentum, and $(j_j)_z$, one of its components. Applying the Wigner-Eckert theorem we obtain

$$\underline{r}_j \cdot (\underline{A}_{Nj} \times \underline{\Gamma}_j) = 2g_N \beta_N (\underline{I} \cdot \underline{j}_j) [\underline{s}_j \cdot \underline{l}_j + s_j^2 - (\underline{s}_j \cdot \underline{l}_j)^2] [r_j j_j (j_j + 1)]^{-1} \tag{A-16}$$
$$= 2g_N \beta_N (\underline{I} \cdot \underline{j}_j)(\underline{s}_j \cdot \underline{l}_j + \tfrac{1}{2}) [r_j j_j (j_j + 1)]^{-1},$$

where we have used the relation

$$(\underline{s} \cdot \underline{A})(\underline{s} \cdot \underline{B}) = \mathbb{1}(\underline{A} \cdot \underline{B})/4 + i(\underline{s} \cdot \underline{A} \times \underline{B})/2 ,$$

valid for spin 1/2 particles.*

---

* To prove this we merely consider the commutation relations,

$$[s_i, s_j] + [s_i, s_j]_+ = i\epsilon_{ijk} s_k/2 + \mathbb{1}\delta_{ij}/4 = s_i s_j$$

Then,

$$s_i A_i s_j B_j = i\epsilon_{ijk} A_i B_j s_k/2 + \mathbb{1} A_i B_i/4 .$$

The above result indicates that in taking spatial average of the last term in (15) we need to evaluate the integral

(A-17) $$\int_0^\infty R^2(r)E(r)\left[1+(E'+e\phi(r))(2m_0c^2)^{-1}\right]^{-2}dr\,.$$

For small r E (r) and ϕ (r) behave like r^{-2} and r^{-1} respectively while the radial part of the wave function R (r) varies like r^l . Hence the integrand is finite but the entire term is small in comparison with the other nuclear term. The contribution is then customarily neglected in the Hamiltonian. When $l=0$ the integrand diverges unless the full denominator is retained (singularity in E is removed by ϕ^2), the integral is now finite and large; in fact one can show that the function

$$f(r)=\frac{eE(r)}{2m_0c^2}\left[1+(E'+e\phi)(2m_0c^2)^{-1}\right]^{-2}$$

has properties similar to those of the Dirac delta function[7]. Away from the origin the denominator is essentially unity. Now $eE(r)$ represents the force acting on the jth electron so the integral of $f(r)$ gives the ratio of electronic energy to $2m_0c^2$, this is of order Kev/Mev. Near the origin $f(r)$ is essentially m_0c^2 which is relatively large. Furthermore, with $E=-\frac{d\phi}{dr}$

$$f(r)=\frac{d}{dr}\left[1+(E'+e\phi)(2m_0c^2)^{-1}\right]^{-1}\;;\;\int_0^\infty f(r)dr\sim 1\,.$$

We conclude that the last term in (15) is significant only for the S-state electrons. On account of its unique spatial property the contribution to the Hamiltonian usually appears in the form $4g_N\beta_N\beta\, S(r)\,(\underline{I}\cdot\underline{S})(3r^2)^{-1}$. By a similar argument, (13)becomes $2g_N\beta_N\beta\, l(l+1)(\underline{I}\cdot\underline{j})[r^3 j(j+1)]^{-1}$, which vanishes for S-state electron. These two terms constitute the magnetic interactions between an electron and the nucleus and give rise to the so-called hyperfine structure. In comparison to electron-electron interactions, in particular the spin-orbit coupling which leads to what is called fine structure in the energy spectrum, the nuclear electron terms are smaller by at least three orders of magnitude.

We now combine the three $(\mathcal{H}_i)_i$ and sum over all electrons to exhibit the total Hamiltonian as

$$\begin{aligned}\mathcal{H} = \sum_i \Big\{ & \frac{P_i^2}{2m_0} - \frac{Ze^2}{r_i} + \sum_k{}' \frac{e^2}{r_{ik}} - e\phi_{ext} + 2Z\beta^2 (\underline{S}_i\cdot\underline{l}_i) r_i^{-3} \\ & + 2\beta^2 \sum_k{}' \Big[-\frac{\underline{P}_i\cdot\underline{P}_k}{\hbar r_{ik}} - \Big\{ (\underline{S}_k \times \underline{r}_{ik})\cdot\underline{P}_i + (\underline{S}_i \times \underline{r}_{ik})\cdot\underline{P}_k \Big\} (\hbar r_{ik}^3)^{-1} \\ & + (\underline{S}_i\cdot\underline{S}_k) r_{ik}^{-3} - 3(\underline{S}_i\cdot\underline{r}_{ik})(\underline{S}_k\cdot\underline{r}_{ik}) r_{ik}^{-5} \\ & - i\{(\underline{r}_{ik}\cdot\underline{P}_i) + (\underline{r}_{ik}\cdot\underline{P}_k)\}(\hbar r_{ik}^3)^{-1} \\ & - \{\underline{S}_i\cdot(\underline{r}_{ik}\times\underline{P}_i) + \underline{S}_k\cdot(\underline{r}_{ik}\times\underline{P}_k)\}(2\hbar r_{ik}^3)^{-1} \Big] \end{aligned} \tag{A-18}$$

$$+\beta(\underline{l}_i+2\underline{s}_i)\cdot\underline{H}_{ext}+2g_N\beta_N\beta\left[\frac{(\underline{I}\cdot\underline{j}_i)\underline{l}_i(\underline{l}_i+1)}{j_i(j_i+1)}+\frac{2(\underline{I}\cdot\underline{s}_i)\delta(r_i)}{3r_i^2}\right]$$

$$-\frac{p_i^4}{8m_0^3c^2}-Ze^2\left[3(\hat{\underline{r}}_i\cdot\underline{R})^2-R^2\right](2r_i^3)^{-1}$$

$$+2\beta^2\underline{s}_i\cdot\left[\underline{E}_{ext}\times\underline{p}_i/\hbar\right]-\beta^2\underline{E}_{ext}\cdot\underline{p}_i/\hbar\Big\}\,.$$

In (18) we have derived a general expression of the Hamiltonian for electrons in an atom. Obviously, any attempt to apply the entire Hamiltonian in a specific problem will be a difficult and tedious task. It is fortunate that for the purpose of discussing electron spin resonance only part of the Hamiltonian will be needed.

APPENDIX B

NUCLEAR QUADRUPOLE INTERACTIONS

In Appendix A a general Hamiltonian for the electrons of an atomic system has been derived. When the system under consideration is subjected to solid state forces and external magnetic fields the description of all the interactions present necessarily has to include effects not involving the electrons. Two such effects of interest in spin resonance studies are the interaction of the nuclear electric quadrupole moment with the crystalline field and the nuclear magnetic dipole interaction with the magnetic field. While the latter interaction is well known and can be written down at once it is perhaps instructive to consider a brief derivation of the quadrupole interaction[42].

Then general interaction between the nucleus, atomic number Z and mass number A, and a crystalline field which gives rise to an electrostatic potential $V(\underline{x})$ can be written as

$$\mathcal{H}_{NC} = \int \rho(\underline{x}) V(\underline{x}) d^3x \,, \tag{B-1}$$

where $\rho(\underline{x})d^3x$ is the amount of nuclear charge in elemental volume d^3x about $\underline{x}$ and integration is over the nucleus. We next expand $V(\underline{x})$ about the nuclear center of mass and obtain as the first two leading terms

(B-2) $$\mathcal{H}_{NC} = ZeV_0 + \frac{1}{2}\sum_{i,j} Q'_{ij} V_{ij} + \cdots ,$$

where $Q'_{ij} \equiv \int x_i x_j \rho(\underline{x}) d^3x$ and $V_{ij} = \left(\partial^2 V / \partial x_i \partial x_j\right)_0$. The first term in the expansion represents the interaction energy of the nucleus treated as a point charge. Since it cannot lead to information regarding nuclear size, shape, or orientation we shall neglect it in subsequent discussions. The next non-vanishing term is the quadrupole interaction to be denoted as $\mathcal{H}_{QC}$.*

Ultimately we will be interested in matrix elements of $\mathcal{H}_{QC}$, where in quantum description, the charge density $\rho(\underline{x})$ is to be regarded as an operator $\rho_{op}(\underline{x}) = e\sum_{k=1}^{Z} \delta(\underline{x} - \underline{x}_k)$. It is known that $\mathcal{H}_{QC}$ is small compared to separation among nuclear energy levels so that only the ground state needs to be considered. This implies that the total nuclear angular momentum will be a constant of motion and all matrix elements will be of the form $\langle Im|\mathcal{H}_{QC}|Im'\rangle$, where m is the magnetic quantum number denoting the projection of nuclear spin $\underline{I}$ along the axis of quantization. Consequently,

(B-3) $$\langle Im|\mathcal{H}_{QC}|Im'\rangle = \frac{1}{2}\sum_{i,j} V_{ij} \langle Im|Q'_{ij}|Im'\rangle ,$$

---

* It can be shown from parity considerations that the nucleus has no electric dipole or octupole moments. The next order interaction not shown in eq. (2) will be that involving the hexadecapole moment.

where

$$\langle Im|Q'_{ij}|Im'\rangle = \int\cdots\int \Psi_I^{m*} Q'_{ij} \Psi_I^{m'} \prod_{s=1}^{A} d^3x_s \,.$$

In this expression $\Psi_I^m(\underline{x}_1,\ldots,\underline{x}_A)$ is the nuclear wave function where $\underline{x}_i$ is the position of the i<u>th</u> nucleon.

In order to obtain the matrix elements of Q'_{ij} we make use of a theorem which states that the corresponding matrix elements of all traceless, second-rank, symmetric tensors are proportional.* The second-rank, symmetric tensor Q'_{ij} is not traceless; however, it can be written as

$$3Q'_{ij} = Q_{ij} - \delta_{ij}\sum_k Q'_{kk} \,,$$

where Q_{ij} has zero trace. The second term is independent of nuclear orientation; it is of no interest in the present discussion and will therefore be neglected. Hence we obtain

$$\begin{aligned}\langle Im|Q'_{ij}|Im'\rangle &\rightarrow \langle Im|Q_{ij}|Im'\rangle/3 \\ &= c\langle Im|\tfrac{3}{2}(I_iI_j+I_jI_i) - I^2\delta_{ij}|Im'\rangle \,,\end{aligned} \tag{B-4}$$

where we have used nuclear spin $\underline{I}$ to construct a second-rank, symmetric, and traceless tensor whose matrix elements are well known. To determine the proportionality constant c we define the nuclear quadrupole moment Q as

---

* For proof not using group theoretical arguments see Ramsey[43]; otherwise see Wigner[44].

$$eQ \equiv \langle II | Q_{33} | II \rangle$$

$$= \int (3z^2 - R^2) \langle II | \rho_{op} | II \rangle d^3R$$

$$= c \langle II | 3I_z^2 - I^2 | II \rangle ,$$

and so

$$c = \frac{eQ}{I(2I-1)} . \tag{B-5}$$

With the foregoing results the part of quadrupole interaction of interest is now written as

$$\mathcal{H}_{QC} = \frac{eQ}{6I(2I-1)} \sum_{i,j} V_{ij} \left[\frac{3}{2}(I_i I_j + I_j I_i) - I^2 \delta_{ij} \right], \tag{B-6}$$

where equality is understood to be in the sense of matrix elements of constant I. The equation can be further reduced by choosing a set of principal axes for the crystalline field, ie., a coordinate system in which V_{ij} is diagnol.

Thus

$$\mathcal{H}_{QC} = \frac{eQ}{2I(2I-1)} \sum_i V_{ii} I_i^2 , \tag{B-6}$$

since V satisfies Laplace's equation. Now if the electric field gradient has axial symmetry,* $V_{xx} = dV_{yy} = -(\frac{1}{2}) V_{zz}$

$$\mathcal{H}_{QC} = \frac{eQ}{4I(2I-1)} (3I_z^2 - I^2) \left(\frac{\partial^2 V}{\partial z^2} \right)_0 . \tag{B-7}$$

---

* If the electric field gradient has spherical or cubic symmetry, then $\mathcal{H}_{QC} = 0$.

This expression is directly derivable from eq. (6) without approximation if one is only interested in diagonal matrix elements (m = m').

We may use the same method in rewriting the electrostatic interaction of nuclear quadrupole moment with the electrons. The matrix elements of this interaction which has been given in Appendix A is

$$\langle Im|\mathcal{H}_{QE}|Im'\rangle = -\frac{e}{2}\sum_i r_i^{-3}\int d^3R\left[3(\underline{R}\cdot\hat{\underline{r}}_i)^2 - R^2\right]\langle Im|\rho_{op}|Im'\rangle. \tag{B-8}$$

Replacing the nuclear coordinates by appropriate spin components, we find again in the sense of equivalent matrix elements for constant I,

$$\mathcal{H}_{QE} = -\frac{ec}{2}\sum_i\left[3(\underline{I}\cdot\hat{\underline{r}}_i)^2 - I^2\right]r_i^{-3}, \tag{B-7}$$

the constant c is determined as before.

APPENDIX C

ANGULAR VARIATION OF THE FINE STRUCTURE COMPONENTS IN AXIAL FIELD

As seen in II-1, the general Spin Hamiltonian in the case of axial symmetric field can be written as

$$\mathcal{H} = \beta \underline{S} \cdot g \cdot \underline{H} + D\left[S_z^2 - \frac{S(S+1)}{3}\right] \tag{C-1}$$

where the electron-nuclear interaction is omitted. This Hamiltonian applies in the case of I = 0, as the example for the even isotope of Cr^{+3} in MgO with a Mg^{++} vacancy in [001] direction (Z-axis here is taken to be the axis of symmetry). With the inclusion of the second term in $\mathcal{H}$, the ESR lines will show the so-called fine structure. The quantity g is in general a tensor with three principal values g_{xx}, g_{yy} and g_{zz}. In the strong field case when $\beta|g \cdot \underline{H}| \gg D$, it is convenient to rotate the coordinate axis so that the first term is diagonal. This can be done by taking the direction of $g \cdot \underline{H}$ as the new Z-axis. The procedure is as follows:

As seen in Figure 23, let $\underline{H}$ and $g \cdot \underline{H}$ make angles (θ, ψ) and $(\bar{\theta}, \bar{\psi})$, with respect to the coordinate axis (crystal axis). We then have

$$H_x = H \sin\theta \cos\psi$$
$$H_y = H \sin\theta \sin\psi$$
$$H_z = H \cos\theta$$

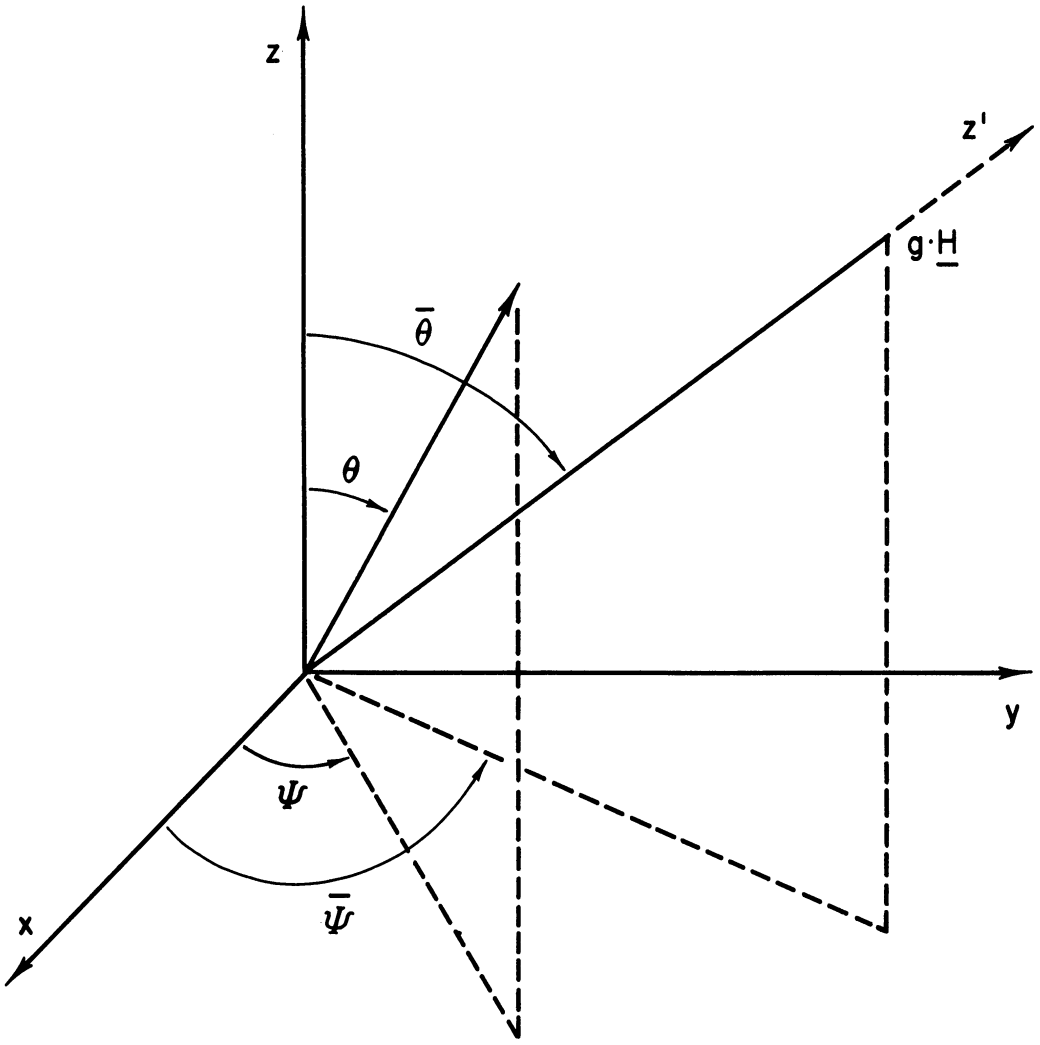

FIG 23

$$(g\cdot\underline{H})_x = |g\cdot\underline{H}|\sin\bar{\theta}\cos\bar{\psi} = g_{xx}H_x = g_{xx}H\sin\theta\cos\psi$$

$$(g\cdot\underline{H})_y = |g\cdot\underline{H}|\sin\bar{\theta}\sin\bar{\psi} = g_{yy}H_y = g_{yy}H\sin\theta\sin\psi \qquad \text{(C-2)}$$

$$(g\cdot\underline{H})_z = |g\cdot\underline{H}|\cos\bar{\theta} = g_{zz}H_z = g_{zz}H\cos\theta$$

From (2) we have

$$|g\cdot\underline{H}|^2 = H^2\left[g_{xx}^2\sin^2\theta\cos^2\psi + g_{yy}^2\sin^2\theta\sin^2\psi + g_{zz}^2\cos^2\theta\right]$$

$$= H^2\left[\left(g_{xx}^2\cos^2\psi + g_{yy}^2\sin^2\psi\right)\sin^2\theta + g_{zz}^2\cos^2\theta\right]$$

Let

$$g_\perp^2 = g_{xx}^2\cos^2\psi + g_{yy}^2\sin^2\psi \quad ; \quad g_\parallel^2 = g_{zz}^2 \qquad \text{(C-3)}$$

and

$$g^2 = g_\perp^2\sin^2\theta + g_\parallel^2\cos^2\theta \qquad \text{(C-4)}$$

We obtain

$$|g\cdot\underline{H}|^2 = H^2g^2 \quad \text{or} \quad |g\cdot\underline{H}| = Hg\,. \qquad \text{(C-5)}$$

Further, from (2) and (5), we also obtain relations between angles.

$$\sin\bar{\theta} = \frac{g_\perp}{g}\sin\theta \quad ; \quad \cos\bar{\theta} = \frac{g_\parallel}{g}\cos\theta \qquad \text{(C-6)}$$

$$\cos\bar{\psi} = \frac{g_{xx}}{g_\perp}\cos\psi \quad ; \quad \sin\bar{\psi} = \frac{g_{yy}}{g_\perp}\sin\psi\,. \qquad \text{(C-7)}$$

Now in axial field with Z as axis of symmetry, $g_{xx} = g_{yy}$, hence from (3)

$$g_{xx} = g_{yy} = g_\perp .$$

Also from (7), $\bar{\psi} = \psi$ that is, $\overline{OZ}$, $\underline{H}$ and $g \cdot \underline{H}$ lie on the same plane, therefore we might as well take this plane to be the X-Z plane (ψ = 0) and rotate the coordinate system around Y-axis for an angle $\bar{\theta}$ so that $g \cdot \underline{H}$ is the new Z' axis, then

$$\beta \underline{S} \cdot (g \cdot \underline{H}) = \beta S_{z'} |g \cdot \underline{H}| = \beta g H S_{z'} ,$$

i.e. the first term is diagonal. Now consider the effect of this rotation on the second term in the Hamiltonian,

$$D\left[S_z^2 - \frac{S(S+1)}{3}\right].$$

The matrix for the rotation can be easily written down in terms of $\bar{\theta}$ as (see Figure 24).

$$\begin{pmatrix} x \\ y \\ z \end{pmatrix} = R_y(\bar{\theta}) \begin{pmatrix} x' \\ y' \\ z' \end{pmatrix} \quad ; \quad R_y(\theta) = \begin{pmatrix} \cos\bar{\theta} & 0 & \sin\bar{\theta} \\ 0 & 1 & 0 \\ -\sin\bar{\theta} & 0 & \cos\bar{\theta} \end{pmatrix}$$

Since $\underline{S}$ transforms like a coordinate under rotation,

$$S_z = -\sin\bar{\theta} S_{x'} + \cos\bar{\theta} S_{z'}$$

or using relation (6) between angle $\bar{\theta}$ and θ ,

$$S_z = -\frac{g_\perp}{g} \sin\theta S_{x'} + \frac{g_\parallel}{g} \cos\theta S_{z'}$$

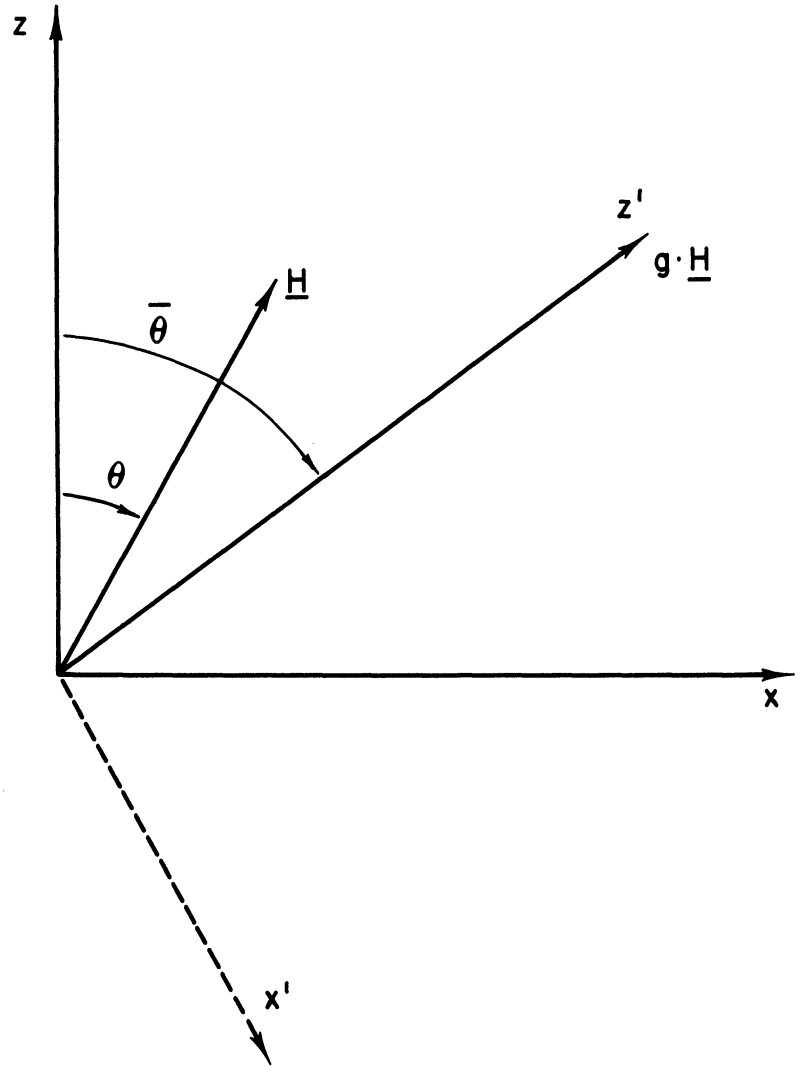

FIG 24

$$= -aS_{x'} + bS_{z'}\,; \quad \text{where} \quad a = \frac{g_\perp}{g}\sin\theta\,, \; b = \frac{g_\parallel}{g}\cos\theta$$

Therefore:

$$S_z^2 = a^2 S_{x'}^2 - ab(S_{z'}S_{x'} + S_{x'}S_{z'}) + b^2 S_{z'}^2$$

or

$$D\left[S_z^2 - \frac{S(S+1)}{3}\right] = D\left[a^2 S_{x'}^2 - ab(S_{z'}S_{x'} + S_{x'}S_{z'}) + b^2 S_{z'}^2 - \frac{S(S+1)}{3}\right]$$

Our Hamiltonian now becomes

$$\mathcal{H} = \beta g H S_{z'} + D\left[a^2 S_{x'}^2 - ab(S_{z'}S_{x'} + S_{x'}S_{z'}) + b^2 S_{z'}^2 - \frac{S(S+1)}{3}\right].$$

For a given S, we can always solve this exactly by setting up matrix for the second term using eigen functions of the first, and then diagonalize it. However, this is unnecessarily complicated by large value of S, and in usual experiment $\beta g H \gg D$ so we can treat the second term as a perturbation. Bleaney[38], Low[39], and Buckmaster[40], have given an expression for this, but here we will show the result to the first order which is sufficient in usual experiments.

Since

$$S_{x'}^2 = \frac{1}{4}(S_+^2 + S_-^2 + S_+S_- + S_-S_+)$$

$$S_{z'}S_{x'} + S_{x'}S_{z'} = \frac{1}{2}(S_{z'}S_+ + S_+S_{z'} + S_{z'}S_- + S_-S_{z'})$$

The second term in the Hamiltonian becomes

$$\frac{D}{2}\left[\frac{a^2}{2}(S_+^2+S_-^2)+\frac{a}{2}(S_+S_-+S_-S_+)-ab(S_{z'}S_++S_+S_{z'}+S_{z'}S_-+S_-S_{z'})\right.$$

(C-10)

$$\left.+2b^2S_{z'}^2+\frac{2}{3}S(S+1)\right]$$

In calculating $\langle M|\ \ |M\rangle$, the first and third terms do not contribute, but

$$\langle M|\frac{a^2}{2}(S_+S_-+S_-S_+)|M\rangle = a^2\left[S(S+1)-M^2\right]$$

$$\langle M|b^2S_{z'}^2|M\rangle = b^2M^2$$

Therefore the energy for given M is

$$E(M)=\beta gHM+\frac{D}{2}\left\{a^2\left[S(S+1)-M^2\right]+2b^2M^2-\frac{2}{3}S(S+1)\right\}$$

$$=\beta gHM+\frac{D}{2}\left\{\left(\frac{g_\perp}{g}\right)^2\sin^2\theta\left[S(S+1)-M^2\right]+2\left(\frac{g_\parallel}{g}\right)^2\cos^2\theta M^2-\frac{2}{3}S(S+1)\right\}$$

$$=\beta gHM+\frac{D}{2}\left[3\left(\frac{g_\parallel}{g}\right)^2\cos^2\theta-1\right]\left[M^2-\frac{S(S+1)}{3}\right]$$

$$E(M)-E(M-1)=\beta gH+D(M-\tfrac{1}{2})\left[3\left(\frac{g_\parallel}{g}\right)^2\cos^2\theta-1\right]$$

or for strong field transition $\Delta M=\pm1$

$$h\nu=\beta gH+D(M-\tfrac{1}{2})\left[3\left(\frac{g_\parallel}{g}\right)^2\cos^2\theta-1\right]$$

or

$$H=H_0-D'(M-\tfrac{1}{2})\left[3\left(\frac{g_\parallel}{g}\right)^2\cos^2\theta-1\right] \qquad \text{(C-11)}$$

where

$$H_0 = \frac{h\nu}{g\beta} \quad , \quad D' = \frac{D}{g\beta}$$

From (11) we see that the fine structure lines are equally separated with separation

$$D'\left[3\left(\frac{g_{\parallel}}{g}\right)^2 \cos^2\theta - 1\right] .$$

Therefore, all the fine structure lines will collapse into one single line at the angle

$$3\left(\frac{g_{\parallel}}{g}\right)^2 \cos^2\theta_0 - 1 = 0$$

i.e.

$$\theta_0 = \cos^{-1}\frac{1}{\sqrt{3}}\left(\frac{g_{\parallel}}{g}\right) .$$

Experimentally, this is a good test for correctness of the Hamiltonian (1) and also a good way to measure $g_{\parallel}$ and hence $g_{\perp}$ after g has been obtained from the position of the single line at $\theta = \theta_0$.

REFERENCES

1. F. Zavoisky, J. Phys. USSR, 9, 211 (1945).

2. R. L. Cummerow and D. Halliday, Phys. Rev., 70, 433 (1946).

3. J. J. Cook, L. G. Cross, M. E. Bair, and R. W. Terhune, Proc. IRE, 49, 768 (1961).

4. D. J. E. Ingram, Spectroscopy at Radio and Microwave Frequencies, London, Butterworths (1955).

5. B. Bleaney and K. W. H. Stevens, Repts. Prog. Phys., 16, 108, (1953).

6. A. Abragam and M. H. L. Pryce, Proc. Roy. Soc., A 205, 135 (1951).

7. J. C. Slater, Quantum Theory of Atomic Structure, Vol. II, New York, McGraw-Hill (1960).

8. C. Kikuchi, Willow Run Report 2616-10-R, University of Michigan (Aug. 1959).

9. L. M. Matarrese and C. Kikuchi, J. Phys. Chem. of Solids, 1, 117 (1956).

10. R. L. Hansler and W. G. Segelken, J. Phys. Chem. Solids, 13, 124 (1960).

11. J. E. Wertz and P. Auzins, Phys. Rev., 106, 484 (1957).

12. C. A. Hutchison, Jr., Phys. Rev., 75, 1769 (1949).

13. A. F. Kip, C. Kittel, R. A. Levy, and A. M. Portis, Phys. Rev., 91, 1066 (1953).

14. G. Feher, Phys. Rev., 103, 834 (1956).

15. G. Feher, Phys. Rev., 105, 1122 (1957).

16. B. S. Gourary and R. J. Adrian, "Wave Functions for Electron-Excess Color Centers in Alkali Halide Crystals", Solid State Physics, Vol. 10, Academic Press.

17. J. E. Wertz, P. Auzins, R. A. Weeks, and R. H. Silabee, Phys. Rev., 107, 1535 (1957).

18. D. R. Speck, Phys. Rev., 101, 1725 (1956).

19. W. Low and D. Shaltiel, Phys. Rev., 115, 424 (1959).

20. T. L. Collins, F. M. Rourke, and F. A. White, Phys. Rev., 105, 196 (1957).

21. D. J. Hughes and J. A. Harvey, 8h. "Neutrons", American Inst. of Phys. Handbook, McGraw-Hill (1957).

22. D. Jowith, S. K. Pattendin, H. Rose, V. G. Small, R. B. Tottensall, AERE, R/R 2516 (1959).

23. R. P. Penrose, Nature, London, 163, 992 (1949); D. J. E. Ingram, Proc. Phys. Soc., A 62, 664 (1949).

24. B. Bleaney, Physica, 17, 175 (1951); B. Bleaney, Phil. Mag., 42, 441 (1951).

25. L. W. Nordheim, Phys. Rev, 78, 294 (1950).

26. C. Kikuchi, M. H. Sirvetz and V. W. Cohen, Phys. Rev, 92, 109 (1953).

27. H. E. Walchli and H. W. Morgan, Phys. Rev., 87, 541 (1952).

28. G. Fricke, S. Penselin, and E. Recknagel, Naturwiss, 4, 129 (1960).

29. G. W. Ludwig and H. H. Woodbury, Phys. Rev. Letters, 1, 16 (1958); Phys. Rev., 113, 1014 (1959).

30. J. W. Orton, Auzins, and Wertz, Phys. Rev., 119, 1691 (1960).

31. G. W. Ludwig, H. H. Woodbury, and R. V. Carlson, Phys. Rev. Letters, 1, 295 (1958).

32. G. W. Ludwig and H. H. Woodbury, Phys. Rev., 117, 1286 (1960).

33. R. W. Terhune, J. Lambe, C. Kikuchi and T. Baker, Phys., Rev., 123, 1265 (1961).

34. J. Eisinger, W. E. Blumberg and S. Geschwind, Bull. Am. Phys. Soc. Series II, Vol. 6, No. 2, pp. 117 (1961).

35. J. Lambe and C. Kikuchi, Phys. Rev., 118, 71 (1960).

36. J. Lambe and C. Kikuchi, Phys. Rev. Letters, 3, 270 (1959).

37. R. S. Title, Phys. Rev. Letters, 4, 502 (1960).

38. B. Bleaney, Phil. Mag., 42, 441 (1951).

39. W. Low, Paramagnetic in Solid State Physics, Suppl. 2, Academic Press (1960).

40. H. A. Buckmaster, Can. Jour. Phys., 39, 1073 (1961).

41. L. I. Schiff, Quantum Mechanics, New York, McGraw-Hill (1955).

42. M. H. Cohen and F. Reif, Solid State Phys., 5, 321 (1957).

43. N. F. Ramsey, Nuclear Moments, New York, John Wiley (1953).

44. E. P. Wigner, Group Theory and its Application to the Quantum Mechanics of Atomic Spectra, New York, Academic Press (1959).

45. H. H. Woodbury and G. W. Ludwig, Phys. Rev., 117, 1287 (1960).

46. A. Abragam, J. Horowitz, and M. H. L. Pryce, Proc. Roy. Soc., A 230, 169 (1955).

47. V. Heine, Phys. Rev., 107, 1002 (1957).

48. J. H. Wood and G. W. Pratt, Jr., Phys. Rev., 107, 995 (1957).

49. R. E. Watson and A. J. Freeman, Phys. Rev., 123, 2027 (1961).

50. K. G. Kessler, Phys. Rev., 79, 167 (1950).